Simulating Open Borehole Hydraulic Cross-Connection in A Multi-Layered Bedrock Aquifer System Informed by High-Resolution Datasets

by

Faran Vahedian

A Thesis

presented to

The University of Guelph

In partial fulfilment of requirements
for the degree of

Master of Applied Science

in

Engineering

Guelph, Ontario, Canada

ABSTRACT

SIMULATING OPEN BOREHOLE HYDRAULIC CROSS-CONNECTION IN A MULTI-LAYERED BEDROCK AQUIFER SYSTEM INFORMED BY HIGH-RESOLUTION DATASETS

Faran Vahedian
University of Guelph, 2021

Advisors:
Dr. Beth Parker
Dr. Jana Levison

Vertical flow in open boreholes is common in fractured rock because the borehole will hydraulically cross-connect the active fractures intersecting the hole. This study uses an equivalent porous medium (EPM) numerical model to examine the effect of hydraulic cross-connection on the flow system and the vulnerabilities surrounding an open borehole cored through the Silurian-aged dolostone aquifer. A suite of high-resolution dataset was used to create a robust site conceptual model (SCM). The numerical model developed from the SCM was shown to reasonably match the field data. The results demonstrate how varying open hole conditions disturb the natural flow conditions leading to erroneous estimation of hydraulic properties and misleading interpretations of data for management decisions. Hydraulic cross-connection caused by open boreholes is important, especially when contaminated sites exist, because these open holes create preferential pathways for re-directing shallow water that moves more readily deeper, increasing the vulnerability of the deeper aquifer.

ACKNOWLEDGEMENTS

I would first like to offer sincere gratitude to Dr. Beth Parker, my primary advisor, for providing continued guidance and support throughout this research journey and for the opportunity to pursue a modeling-based research topic that truly interests me. Her lifelong contributions to field-focused groundwater research, education, and practice are impressive and I am so grateful for the opportunity to have worked with a remarkable team of researchers and students at the Morwick G^{360} Groundwater Research Institute.. I would like to thank my co-advisor, Dr. Jana Levison who was always supportive and patient. Thank you Jana for the consistent feedback, valuable insights on my research, and helpful reviews of this work. Jana's trust in my abilities opened a door to me to work with the G^{360} group and I will never forget that. Additionally, I would like to thank Gaelen Merritt for offering his invaluable knowledge of novel applied groundwater modeling and valuable insights from a different perspective on my work. Working with Gaelen made this modeling adventure even more exciting.

A big thank you to all the G^{360} researchers and students who made this journey possible. I am incredibly grateful for the expertise and support of Dr. Patryk Quinn, Dr. Jonathan Munn, Dr. Pete Pehme, Andrew Stockford, Chrystyn Skinner, and Teresa Pilato for data collection and analysis and valuable insights on the project. I would like to extend my gratitude to my friend Elisha Persaud for her perspective on hydrogeological modeling and also emotional support. Thank you to my G360 friends, Teresa, Chrystyn, Andrew, and Glen who made my life in Guelph more enjoyable since the start of the pandemic.

I am incredibly grateful for the friends who have supported me throughout this experience. A big thank you to my best friend, Farid joon, and his dog, the queen of beauty, Miss Lexie. Farid, your unconditional support of my goals and great advice on my current and future life mean the world to me and I cannot thank you enough for what you have done for me during the last 3 years. Thank you, Parisa, my sister, not by blood but by heart who taught me to always believe in myself.

I would like to acknowledge that this research is reliant on numerous studies conducted on land rich in Indigenous history and home to many First Nations, Inuit, and Metis people today, with much respect to those who knew these lands long before. Finally, the numerical model of this study was developed using FEFLOW. I would like to acknowledge the DHI company for providing this study with a free FEFLOW license and all the support throughout the journey.

I dedicate this degree to my family. To my mom, for making my immigration story possible in the first place and for being always supportive of my adventures and dreams. Maman Lila, your trust in my ability is the reason why I am here and I adore you. To my brother, Farshid, who showered me in the endless love and support, you know you are the light of my life. It's been three years since we were together and I hope I can see you and mom very soon. Finally, to my father, who is not between us anymore but I can always feel his soul right by my side.

TABLE OF CONTENTS

LIST OF TABLES

LIST OF FIGURES

Introduction

1.1 Background

Groundwater is a vital resource, with worldwide dependencies upon this supply for drinking and sanitation. About 30 percent of the Canadian population and 28.5 percent of the population in Ontario use groundwater, with this number much higher (90 percent) in rural areas (Dewar & Soulard, 2010; Taylor et al. 2009). In southern Ontario, the main sources of groundwater used by numerous communities are the underlying fractured sedimentary bedrock aquifers and the Silurian dolostone aquifer along the Niagara Escarpment from Niagara Falls to the Bruce Peninsula (Johnson et al. 1992; Steelman et al. 2017) serving approximately 1M people. Fractured sedimentary bedrock aquifers contain features that enhance flow such as fractures (e.g. joints and bedding partings) and vuggy porosity within the porous rock matrix, creating a complex network of preferential flow features (Bear, 1993; Berkowitz, 2002; Neuman, 2005; Munn, 2019). In 2006, following the Walkerton Tragedy, the Clean Water Act was introduced in Ontario to protect sources of drinking water, which included assessment of groundwater vulnerability. Under this program, a regional groundwater flow model, developed through the “City of Guelph Tier Three Water Budget and Local Area Risk Assessment” was used to delineate wellhead protection areas (Matrix Solutions Inc., 2017).

Fractures act as preferential pathways in rock (Berkowitz, 2002), and their connectivity influences groundwater flow pathways. Meyer et al. (2008) showed that the joint terminations at bedding planes may explain the head loss within fractured sedimentary rock aquifers influencing hydraulic head distributions, and showing that aquitards can be much thinner and often do not align with lithostratigraphic unit boundaries. Fracture and matrix data from site characterization studies can be used to inform discrete fracture matrix (DFM) numerical models to represent plume migration where the number and aperture of hydraulically active fractures influence bulk plume migration rates or travel times and fluxes to receptors (Chapman et al. 2013; Parker et al. 2018; Pierce et al. 2018; Pilato, 2021). These studies provide support for using a suite of discrete fracture network and matrix (DFN-M) methods (a selection of field and laboratory methods on core and in the borehole) to enhance the hydrogeological characterization of fractured sedimentary bedrock aquifers (e.g., dolostone) with porous rock matrix blocks between fractures through acquisition of high-resolution field data (Parker et al. 2012). Highresolution datasets are the basis to develop hydraulically-informed, processbased SCMs through delineation of hydrogeologic units (HGUs) “which are partitions of groundwater flow system with contrasting hydraulic conductivities and vertical gradient” (Poeter and Gaylord, 1990; Parker et al. 2012; Meyer et al. 2008, 2014, 2016) to build robust numerical simulations to predict groundwater flow and contaminant transport. Vertical flow in open boreholes has been observed as far back as the 1950’s in boreholes that intersect multi-layered aquifer systems. This vertical flow is caused by the differing heads in the units, where water enters the hole from the units with higher head than the blended head, and exits the hole through the units with lower head. Sokol (1963) was

one of the first researchers to mathematically describe the relationship between the blended head in the open hole and the individual heads in multiple aquifers intersected by the well. Researchers in the late 1980s-1990s were able to infer vertical flow from the chemical analysis of groundwater samples collected throughout the open hole water column (e.g., Reilly et al. 1989; Williams and Conger, 1990; Brassington, 1992; Church and Granato, 1996; Shapiro, 2002). Price and Williams (1993) inferred cross-connection affecting the natural groundwater chemistry by comparing pore water analysis to samples collected in specific portions of the hole isolated by straddle packers. Sterling et al (2005) described in detail cross connection effects on the TCE distributions by comparing rock core concentrations to groundwater samples from a multilevel system. Flow metering in open holes under pumping and abient conditions has long been used to identify the most permeable zones (e.g., Hess, 1986; Paillet, 1998, 2000, 2001). Others have used salinity differences of the borehole water to identify flow (e.g., Tsang et al, 1990) and dilution methods with active logging have been shown to produce similar results (e.g., Pitrak et al. 2007). Keller et al. (2014, 2017) presented a method to obtain a transmissivity profile by sealing boreholes after drilling with a flexible liner and measuring the liner descent velocity, and if the liner is sequentially removed, a head profile can be obtained. More recently, others have used the FLUTe technology to seal boreholes and identify ambient flow through temperature logging (e.g., Pehme et al 2013) or use the liner to seal a string of transducers against the borehole wall to obtain a hydraulic head profile (Pehme et al. 2014) or seal fiber optic cables against the wall to characterize ambient flow (Coleman et al. 2015; Maldaner et al. 2019; Munn et al. 2020).

Even though considerable research has been done to understand the effects of hydraulic cross-connection in boreholes, only a few studies simulated the effects of cross-connected systems (Myers, 2019; Poulsen, 2019) with the focus on contaminant transport. This study builds off of this work by starting with a numerical model of a multilayered fractured dolostone aquifer that is calibrated and PEST optimized to represent the regional flow system partially informed by high-resolution data. Then the local conditions around a cross-connecting borehole together with DFN-M field datasets are used with a cutout of the regional model to refine the local flow system conditions in order to quantify borehole cross-connect effects throughout the vertical profile.

Groundwater modeling can be a useful tool to investigate the impacts of crossconnections. Groundwater flow is often modeled using the ‘equivalent porous medium’ (EPM) approach, assuming that the fractures are sufficiently numerous and wellconnected and that the hydraulics of the fractured aquifer system can be reasonably represented using porous media bulk parameters (Berkowitz et al. 1988). Despite the simplifications, the EPM approach generally provides satisfactory results representative of the groundwater flow system although it is much more challenging to represent contaminant transport (Guerin and Billaux, 1994; Carneiro 2005; Chapman et al. 2014). A hybrid EPM-DFN approach is recommended for numerical modeling of groundwater flow with contaminant transport, where the EPM model is used to simulate the flow system conditions where hydrogeologic units have well-define parameters and transport is modeled using the DFM approach (Chapman et al. 2014). In this study, FEFLOW is

used to develop an EPM model that is refined using the DFM datasets requiring a methodology to bridge the gap between these methods in order to illustrate the dynamic hydraulic flow in and out of the open borehole.

1.2 Thesis Objectives

The main goal is to develop a steady-state EPM numerical model informed by field data to examine the effects of open borehole hydraulic cross-connection on the flow system and the vulnerabilities surrounding a single 85 m deep borehole cored through the multiple members of the Silurian-aged dolostone aquifer. It is evident that hydraulic cross-connection occurs in the borehole under the open hole condition and hypothesized that the flow system is altered in a variable way at different depths depending on the blended well and natural system conditions. At this study site, the redistributed flow conditions are variable with depth and contributing to bedrock aquifer vulnerability in deeper zones to shallow and surface sources of contamination, not previously quantifie. The 3D EPM model representing a multi-layered fractured aquifer system is designed to evaluate hydraulic responses in the flow regime and changes in flow direction/velocity field (particle tracking) for the study site field conditions, and visually demonstrate the changes in flow conditions with depth and illustrate through scenario testing, the range of impacts on potential contaminant transport pathways (relation of recharge or contaminant sources to plume receptors) and vulnerabilities created by various open borehole configurations.

The thesis is organized into four sections. This introductory chapter starts with a literature review of relevant field characterization and modeling methods used to support the study and continues with thesis objectives and scope. Chapter 2 introduces the approach and methodology. Insights from the field data and pre-existing studies are combined to develop the 3D EPM flow model to simulate the effects of open borehole hydraulic cross-connection. Chapter 3 discusses the results and the implications of hydraulic cross-connection using hypothetical scenarios along with the study limitations and recommendations for future work. The overall conclusion is presented in Chapter 4. Finally, the Appendices contain other findings that may be of interest for this study, including more details on the interpretation of the high-resolution data, distribution of the model inputs, model outputs, and the regional model.

2 Approach and Methods

The issue of hydraulic cross-connection in boreholes with long open well screens is of universal interest. It is a common practice to use blended heads over open borehole (or long screened) intervals as opposed to depth-discrete heads over shorter intervals to represent the hydraulic head under ambient conditions. This causes potential sources of error for the investigation of groundwater systems and evaluation of these impacts is important to better understand groundwater system behavior, ultimately to aid decision-making. This investigation uses a well-studied Silurian dolostone aquifer underlying the City of Guelph, Ontario, Canada as a realistic field scenario to demonstrate the influence of open (or long screened) boreholes on the flow paths from recharge to discharge areas and the seriousness of these effects in an urban hydrogeologic setting. The Guelph aquifer has been subject to intensive research investigations, characterization, and monitoring datasets for many years (Kennel, 2008; Belan, 2010; Munn, 2012; Fomenko, 2015; Munn, 2019; Skinner, 2019; Johnson, 2020; Pilato, 2021). There is

The existing 3D EPM flow model for the greater Guelph area (Matrix Solutions Inc., 2017) was used to inform the boundary conditions and initial framework of the study area flow model. The approach was to refine the “cutout ” (subregional scale- a smaller domain within existing calibrated, optimized model with consistent boundary conditions) based on the site-specific information for the Guelph aquifer where sufficient high-resolution data are available to represent the field conditions around HBP5 as best as possible using a stylized model. Similarly detailed data from additional boreholes were relied upon to create the cutout flow model better representing the site conditions. Then, the 3D EPM model was used to evaluate, quantitatively, the influence of various length boreholes on vertical cross-connection.

Therefore, this study is comprised of two main stages: 1) collection and interpretation of high-resolution data from HBP5 (the study borehole) along with the pre-existing data from other boreholes within/near the research area (Figure 2-2:C shows the locations where high-resolution data are available); and 2) the numerical model development for a cutout area or subregion of an established, calibrated and parameterized 3D EPM flow model, whereby these field data were used to refine the subregion then used to develop the revised EPM model for the study area subdomain model (Figure 2-1:).

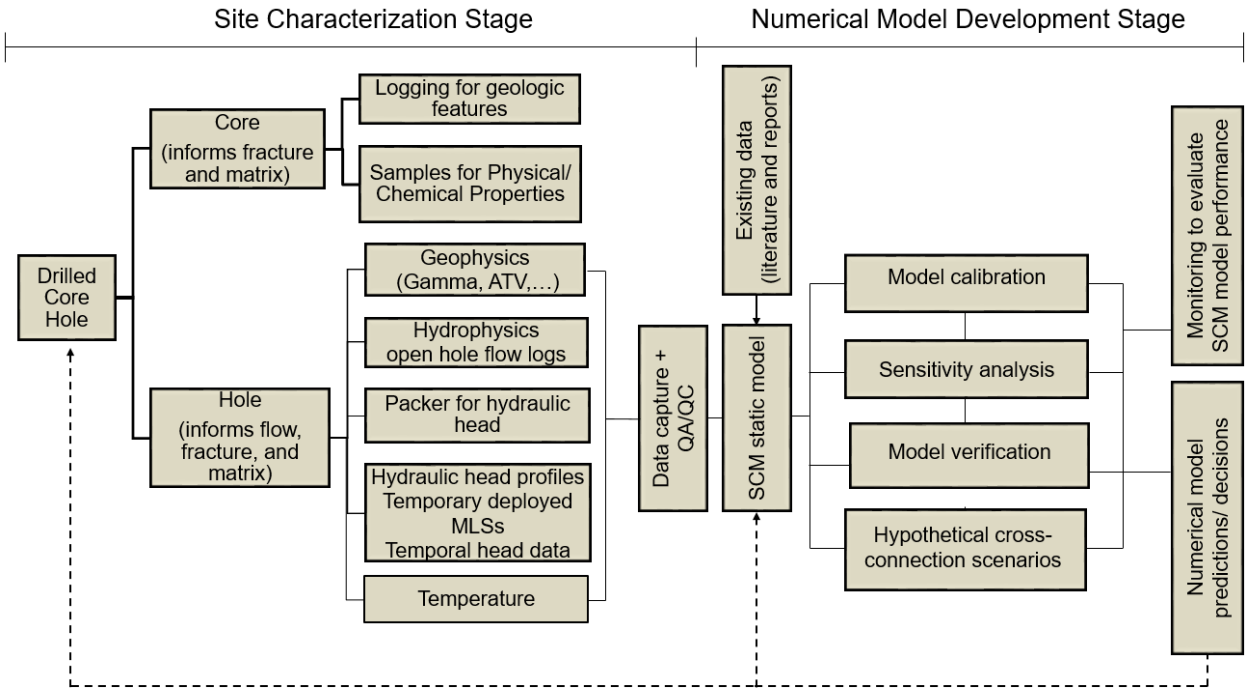

Figure 2-1: The flowchart summarizes the two main stages of the study.

2.1 Site Description

The research domain has areal extent of 100 km^2 and is situated within the City of Guelph in southern Ontario where a population of approximately 130,000 relies on groundwater resources (using a well-field of 21 operating wells) for its potable water supply (Figure 2-2:C). This resource, known as an excellent source of freshwater (Singer et al. 2003), is primarily drawn from a fractured Silurian dolostone aquifer system (Figure 2-2:A) that extends along the Niagara Escarpment from Niagara Falls to the Bruce Peninsula. The regional stratigraphic sequence in the Guelph area is subdivided into eight geologic Formations (Figure 2-3) including Guelph (the uppermost Formation), Eramosa, Goat Island, Gasport, Irondequoit, Rockway, Merritton, and Cabot Head (the lowermost Formation) (Brunton and Britnell 2011). Eramosa Formation is subdivided into three members (Vinemount (V), Reformatory Quarry (RQ), and Stone Road (SR)), and the Goat Island Formation has two members: Ancaster (A) and Niagara Falls (NF). The City of Guelph depends upon the Guelph and Gasport Formations for drinking water supply. The former Formation is known as the main unconfined aquifer and the latter represents the main confined aquifer due to the high transmissivity of the limestone unit. These two aquifers are separated by two discontinuous shaley dolostone formations: Eramosa and Goat Island. The Eramosa and Cabot Head Formations are known as regional aquitard units (Nunes et al. 2021; Brunton, 2008, 2009).

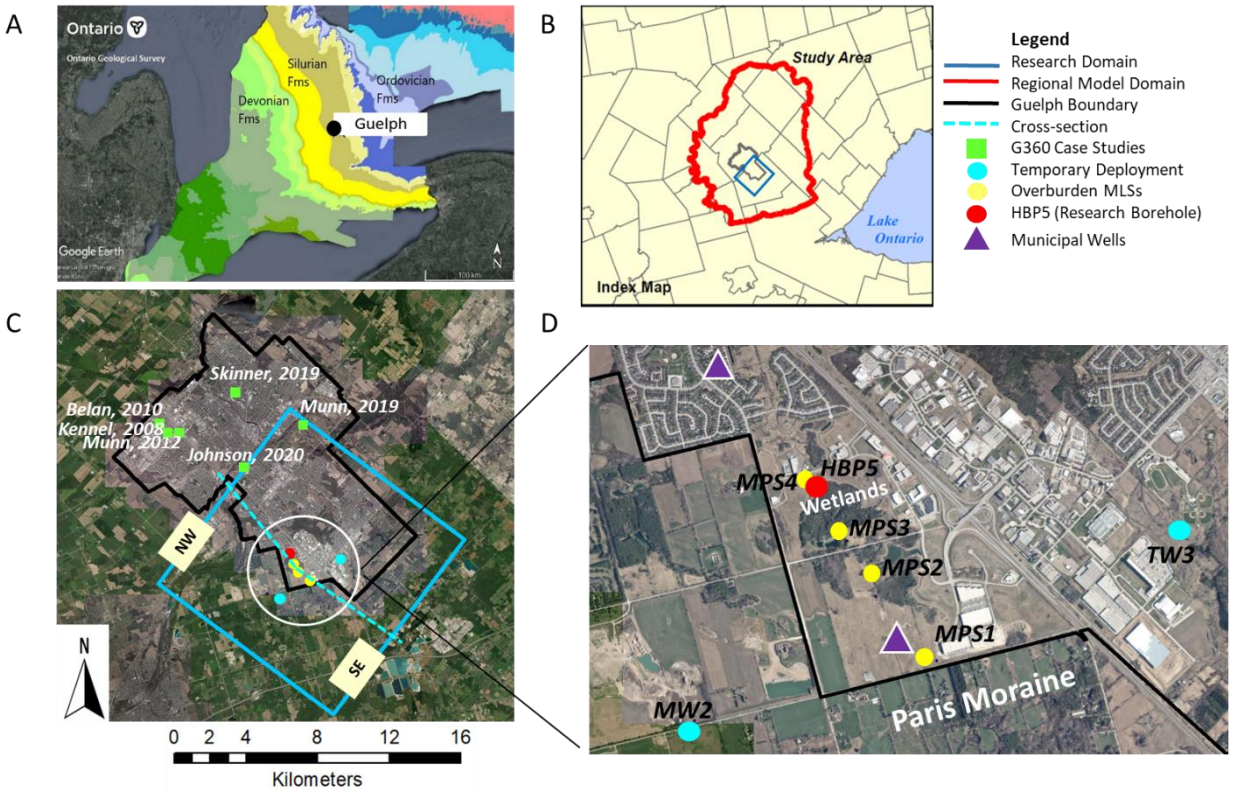

Figure 2-2: (A) Guelph location within the regional geology, (B) the regional model domain, the City boundary, and the research model domain (modified from Matrix Solutions Inc., 2017), (C) the pre-existing advanced characterization studies conducted within the Guelph area, (D) high-resolution monitoring boreholes within the research domain.

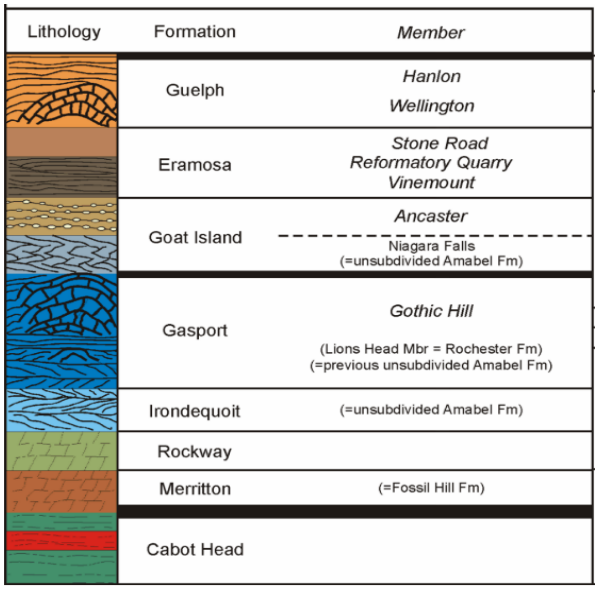

Figure 2-3: The Brunton (2009) framework for the stratigraphy of southern Ontario Silurian rock

The surficial geology comprises primarily glaciofluvial outwash, sand and gravel, and deposition of till materials, including Catfish Creek Till, Mary Hill Till, Wentworth Till, and Port Stanely Till with different scales of heterogeneity (Arnaud et al. 2018). Some zones behave as confining units that reduce leakage to the lower units while the permeable materials such as sand and gravel allow for higher groundwater flow and connect regionally providing recharge to the underlying bedrock. Local relief ranges approximately from 345 to 315 m above sea level (m asl) throughout the research domain (Matrix Solutions Inc., 2017). Surface topography elevates (~340 m asl) along the Paris moraine in the southeast and slowly decreases toward the Speed River in the Northwest boundary (~316 m asl). Regional shallow groundwater flow follows the topography trend (toward the northwestern boundary due to the influence of the Paris moraine) while local groundwater flow is more dominated by pumping of the supply wells across the city. The mean annual precipitation is 921 mm (Environment Canada, 1976-1979)

The research domain was selected given the recent drilling of high-resolution monitoring well “HBP5” located near a new water supply well to support future demands for the City of Guelph. During drilling, it was discovered that there were dramatically varying hydraulic heads in distinct depth horizons. The Paris moraine crossing the southeastern boundary of the City (Figure 2-2:D) is characterized by a belt of hummocky topography, consisting primarily of diamict (till) (Arnaud et al. 2018). Extensive outwash plains (sand and gravel deposits) are located both in front (northwest boundary) and behind (southeast boundary) of the moraine. The water table elevation is higher in the moraine (~8 m) than in the discharge areas (wetlands) located in the vicinity of HBP5. Geology and topography control the groundwater to rise above the ground surface, causing a flowing artesian condition in HBP5. This condition starts at 21.3-23.6 m below ground surface (m bgs) where the zone is sandwiched between the upper Guelph Formation above it and the Reformatory Quarry of Eramosa Formation below it, pressurizing it to the point of it being a flowing artesian zone (i.e. forcing the groundwater level to flow from the artesian zone to the non-artesian zone and rise above the ground surface). Artesian flow significantly slows within the Goat Island Formation (36.5-38.9 m bgs). Furthermore, in the Gasport aquifer, the heads are lower than the shallow system in part due to pumping from municipal supply wells. These are the main components leading to a strong head difference between the shallow system and the deeper aquifer “Gasport” at the HBP5 location.

2.2 DFN-M Field Approach

The site characterization completed within the research domain follows the DFN-M field approach developed by Parker et al. (2012). This approach emphasizes the acquisition of the complementary datasets in vertical profile from both the rock core and borehole in fractured bedrock system. Accurate data describing the behavior of the aquifer system rely on the high-resolution DFN-M techniques that provide multiple lines of evidence for hydrogeologic characterization of the subsurface system.

A robust suite of geological, geophysical, and hydrophysical techniques was deployed at HBP5. The DFN-M approach began with coring a hole in HBP5. The continuous core was completed using S Geobor (SG) wireline rotary coring technique with water as the drilling fluid which creates a 6.625" diameter borehole (~85 m deep). The casing depth is 14.3 m (the top of the casing (TOC) is 0.5 m above the ground surface). Rock core sampling was completed (23 physical properties samples and 48 chloride samples were collected) to provide insight on transport properties of the matrix and understanding the existing contaminant(s) (Kennel, 2008; Munn, 2012; Fomenko, 2015; Skinner, 2019; Hommersen, 2021) to contribute to the rock matrix properties database for the regio and existing data was used in this study. Continuous core logging provided foundational information on lithologic and fracture features such as depth, frequency, and orientation, colour, mineralogy,grain size and cementation.

After coring, three open hole geophysical logs including natural gamma, acoustic televiewer (ATV), and Thermal Vector Probe (TVP) were conducted in HBP5 to provide complementary insight into the stratigraphic sequence and the fracture network (Parker et al. 2012). Natural gamma measures the mineralogy of the rocks (particularly potassium in clay and shale). ATV generates a borehole image and measures the amplitude and travel time of the acoustic signal reflected off the borehole wall which is affected by the characteristics of the wall (hardness and structure). TVP, a multi-sensor probe (four sensors), is another advanced high sensitivity technique used to measure both the temperature and the characteristics of the thermal gradient. This information can be used to measure the horizontal and vertical components and direction of the thermal gradient along the length of the borehole and thereby monitor the temperature recovery and determine the thermal subunits in the borehole based on the orientation and/or magnitude. The TVP data provide additional lines of evidence into the groundwater flow within the fractured rock (Pehme et al. 2014). A down-hole video log was also recorded in the borehole.

Hydrophysical techniques were performed at HBP5 to better understand the hydraulics of the aquifer system including straddle packer hydraulic measurement and flowmeter logging using impeller, and heat pulse. Straddle packers were used to measure a depth-discrete head profile in a partially open hole (Price and Williams 1993; Quinn et al. 2012; Quinn et al. 2016). For HBP5, four packers (deflated diameter: 3.35”; inflated diameter: 6.38”; length: 25-40”) were used to create three short intervals (1.5 m) to collect head values at three zones at the same time throughout the borehole. The straddle packer system measured the hydraulic head of the isolated intervals while the rest of the borehole remained open. This system was inflated nine times at different depths to obtain head profiles throughout the borehole with transducers placed in each interval between the packers. Positive vertical gradients on the packer head profile are evidence of upward flow and negative values show downward flow.

Flowmeter testing measures the cumulative vertical flow continuously across open boreholes and determines zones contributing to the flow into/out of the borehole (Paillet, 2000; Wilson et al. 2001). HBP5 was entirely tested with the impeller flowmeter and the

lower and upper portions with the heat pulse flowmeter where the flow condition is ambient. The test was conducted following standard industry practice as recommended by the manufacturer and completed in a narrow time window immediately after the packers were removed to restrict strong vertical flow within the open hole, minimizing the vertical cross-connection. The impeller measures the velocity of water movement relative to the probe (either stationary or moving) based on the spin of the impeller without resolution of direction. The impeller probe can only measure flow above a threshold that varies depending on whether the flow is downward passing the probe or upward directly into the impeller. Four dynamic tests were conducted, two with the probe moving down the hole and two moving upward, nominally at 2 and 4 m/min in each direction. The relative changes in flow patterns from the flowmeter logging showed excellent repeatability in four different logs, although conditions had not reach steady state. The Heat pulse testing measures the directional flow rate by forcing the water movement through the probe with baffles and measuring the time required for a pulse of heat to travel vertically between a heater and thermistors above and below. Twenty-seven stationary tests were conducted (at each depth a minimum of 3 and a maximum of 6 repeated measurements).

Multilevel systems (MLSs) measure depth-discrete hydraulic heads in granular and fractured environments. Four (6 in) G360 MLSs (MPS1-4) were installed in the overburden within the research domain to complement the existing conventional network. These systems were developed by researchers from the Morwick G360 Institute for Groundwater Research at the University of Guelph (2019, 2020). Lithostratigraphic log, natural Gamma, and head profiles derived from these systems were used to inform/refine the overburden hydrogeologic layers represented in the cutout .

A temporary deployment of transducers for obtaining a high-resolution temporal vertical head profile is another DFN-M technique that monitors the pressure in bedrock boreholes. Transducers were deployed in two bedrock boreholes within the study area (MW2 and TW3) which were sealed using FLUTe^{TM} liners (Pehme et al. 2014). In MW2 (6-in borehole), 26 transducers were deployed along a string at locations of interest, each with a vertical interval ranging from 0.5 to 1 m and a 1-second sampling interval, and 22 transducers were placed in TW3 (8-in borehole) with a vertical interval ranging 0.5-1.5 m and a 1-second sampling interval. All transducers were calibrated to allow the assessment of vertical gradients (Pehme et al. 2014).

2.3 Numerical Model Methods

The conceptual model layers are based on hydrogeologic units that were well-established for the bedrock by other documented studies conducted in the Guelph area using advanced field characterization methods (Belan, 2010; Munn, 2012; Munn, 2019; Skinner, 2019; Johnson, 2020) as described by Meyer et al. (2008) where the positions of HGU boundaries were primarily gleaned from the inflections on the head profiles and

complimented by comparison of corroborating datasets (such as lithostratigraphic and gamma logs). The study model extends from the ground surface to Cabot Head Formation and features 12 HGUs in the bedrock representative of a multi-layered aquifer-aquitard system.

Understanding of the Guelph aquifer system has also been advanced by a 3D steady-state EPM flow model at the larger regional scale (Matrix Solutions Inc., 2017) using FEFLOW (simulation tool) and PEST (calibration tool). Figure 2-2:B shows the boundary of the regional model which was used to inform/constrain the "cutout " model of the focused study area presented herein. Of the prevalent commercial software, this study uses FEFLOW, a finite element subsurface flow simulation system, to be consistent with the regional model (Matrix Solutions Inc., 2017) but more importantly because it has advanced capabilities to represent the complexity of groundwater flow in porous media (Chapman et al. 2014; Frind and Molson, 2018; Moeck et al. 2020) and the groundwater flow and conduit-matrix interactions in fractured media (Diersch, 2013). A steady-state model is used to be consistent with the regional model (Matrix Solutions Inc., 2017) that informs the cutout model boundaries. The steady-state assumption allows for modeling borehole cross-connections and therefore, the extra computational load of transient modeling is not essential to fulfill the purpose of the study. The closest pumping well used by the City of Guelph is located 1.5 km away (to the north) from HBP5 (Figure 2-2D). Hydrographs from HBP5 multi-packer system (Stockford, in progress) showed that the radius of influence of the municipal well impacts the HBP5 location. However, the maximum recovered head value when the supply well was inactive was used in the modeling process to represent pseudo steady-state non-pumping conditions.

The SCM (100 km^2 domain; ~85 m deep) defined as a heterogeneous and anisotropic system with 15 layers (12 in bedrock plus 3 in overburden) was informed by a combination of high-resolution vertical head profiles and lower resolution borehole datasets in the bedrock and overburden within or near the study area. The multilevel high-resolution datasets are the keys to a revised SCM that was partially included in the source water vulnerability study (Matrix Solutions Inc., 2017). The top layer of the flow model corresponds to the Digital Elevation Model (DEM) of the site (resolution of 30 m×30 m) representing the ground surface. The model domain was discretized into triangular mesh with 131,274 elements and 71,876 nodes in total with the grid refined around observation points. The meshes were refined around the boreholes to a nodal spacing of ~ 2 meters where a higher resolution of model output is desired. Local refinement was made where needed to ensure a better mesh quality by checking for obtuse angles and triangles violating the Delaunay and the Péclet Number criteria (Diersch, 2013).

The research domain is bounded by two dominant hydrological features: Speed River (northwestern) and Mill Creek (southeastern) acting as specified head (SH) boundaries. The nodes along these boundaries (Figure 2-4:) were assigned to specified heads informed by the regional study (Matrix Solutions Inc., 2017). The eastern and western boundaries are set to be no-flow boundaries because they are parallel to the groundwater flow lines from the regional potentiometric map. Half of the eastern boundary in the

overburden was set to specified head values to simulate the regional flow pathways. A range of 295 to 330 m asl was assigned to the specified head nodes which correspond with the potentiometric surface from the regional model. Recharge is driven by the regional gradient, entering the system mainly from uplands (Paris moraine) and moving laterally or staying pressurized by the regional aquitard (Arnaud et al. 2018). The distribution of recharge rates was relatively in agreement with the regional recharge map (AquaResource, 2009a). A range of 5-250 mm/y was assigned to the top layer as the initial recharge rates. The highest recharge value was assigned to the hummocky areas (250 mm/y) while the lowest value (5 mm/y) was assigned to the wetlands. Figure 2-4: shows the boundary conditions on a plan view on the top layer. Bulk hydraulic conductivity (K_b) values were initially informed using the pre-existing K_b values indirectly estimated from packer testing with the University of Guelph packer testing equipment in boreholes within the City (Belan, 2010; Quinn et al. 2011; Meyer et al. 2014; Skinner, 2019; Johnson, 2020), and the calibrated K_b values from the regional study. The horizontal K_b values ranging from 8E-03 to 1E-10 m/s initially assigned to the SCM were slightly changed later during the calibration process. To represent the artesian condition across a specific depth at the HBP5 location, the hydraulic gradient of the whole layer (where artesian condition starts) needed to be pressurized. Thus, higher values of specified head and hydraulic conductivity needed to be assigned to that unit than the other layers. Given the nature of finite element models, the EPM layers must be continuous across the domain, and therefore, a minimum thickness of 0.5 m was assigned to short intervals or delineated surfaces with distinct behavior identified by Skinner (2019) and Johnson (2020).

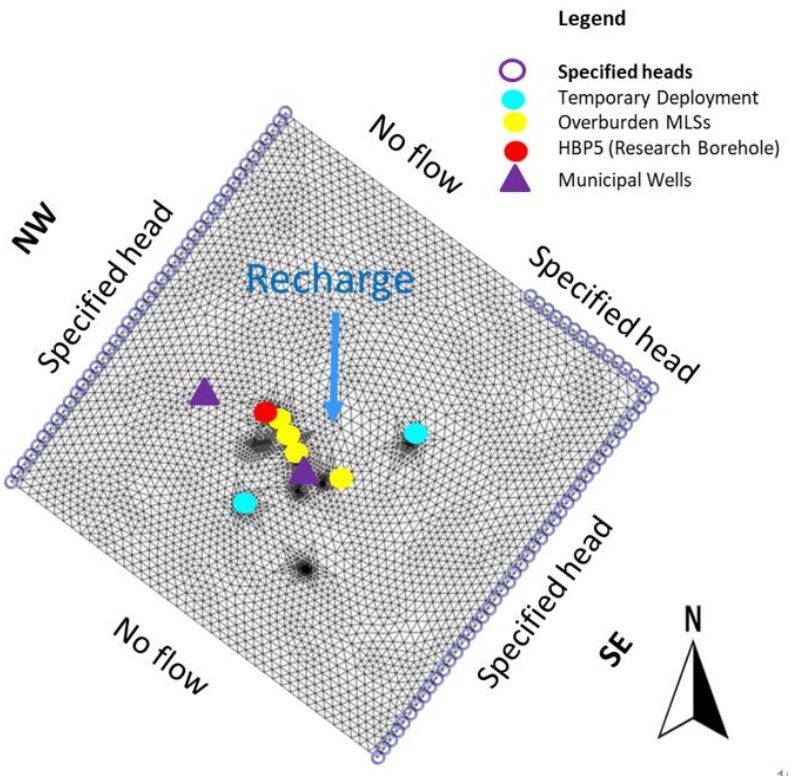

Figure 2-4: The boundary conditions on the top model layer. Densely spaced nodes show the locations of the boreholes.

The steady-state EPM model (with no open borehole) was calibrated to 40 depth discrete head points from seven boreholes (straddle packer hydraulic measurements at HBP5, four overburden MLSs (MPS1-4), and two temporary deployments at TW3 and MW2) distributed across the research domain (Figure 2-2:D). Iterative manual calibration was used to accomplish a satisfactory match between predicted and measured head values. To examine the key sources of uncertainty in the conceptual model, a relative sensitivity analysis of input parameters (hydraulic conductivity, recharge, specified head) was conducted with respect to the calibrated input parameters using the objective function value given by:

$$RS = \frac{1/n \sum_{i=1}^{n} \frac{(H_i - H_{ref})}{H_{ref}}}{1/m \sum_{i=1}^{m} \frac{(P_i - P_{ref})}{P_{ref}}} \qquad \textit{Eq. 1}$$

where RS is the relative sensitivity coefficient (−) averaged over the number of observations, H_i is the simulated value at observation point i with the modified parameter value P_i, and H_{ref} is the reference simulated output at observation point i with the reference

parameter value P_{ref}. The lower the RS, the more robust the model while the larger value represents greater parameter sensitivity (McCuen, 1973; Persaud et al. 2020). Variations of 1-3 orders of magnitude to the K_b values and ± 10% and ± 30% to recharge rates were applied (Levison et al. 2014). Thus, all the elemental values were shifted in each iteration. An offset of ± 1-2 m was applied to the specified head nodes allowing for the evaluation of how the aquifer system is controlled by this parameter.

The open borehole condition has been simulated in MODFLOW using the MNW[1] package to examine contaminant transport pathways through open boreholes from hydraulically fractured shale to a near-surface aquifer (Myers, 2012) and to quantify sample bias caused by intraborehole flow in long screened wells in a homogeneous aquifer (Poulsen et al. 2019). This study focuses on the simulation of the flow re-distribution and the potential vulnerabilities as a result of introducing hydraulic cross-connection to the subsurface system. A 1-D discrete elemental feature/conduit using the Hagen-Poiseuille equation (Eq. 2) with laminar flow assumptions in a circular tube, was used to simulate open borehole cross-connection within the EPM domain in FEFLOW.

$$Q_{pipe} = VA = \frac{gd^2A}{32vL}\Delta h \qquad \textit{Eq. 2}$$

Where Qpipe is the flow through the pipe, d is the diameter of the pipe, g is the acceleration due to gravity, L is the length of the pipe, A is the cross-sectional area of the pipe, and v is the kinematic viscosity of the flowing fluid; and ∆h is the head loss. The line element functions as a conduit that distributes the hydraulic head and flow along the borehole, disturbing the natural flow pattern in the system. A small area around HBP5 was selected on each layer across the screened section (Figure 2-5). The subdomain budget in FEFLOW separates “discrete features”. The masked area can only affect the “flow across the discrete feature component” through discretization error (i.e., if a huge area is selected around the borehole because of insufficient mesh refinement, a different calculated flow through discrete feature can be obtained due to the discretization issues) (Matrix Solutions Inc., 2017).

[1] Multi-node well

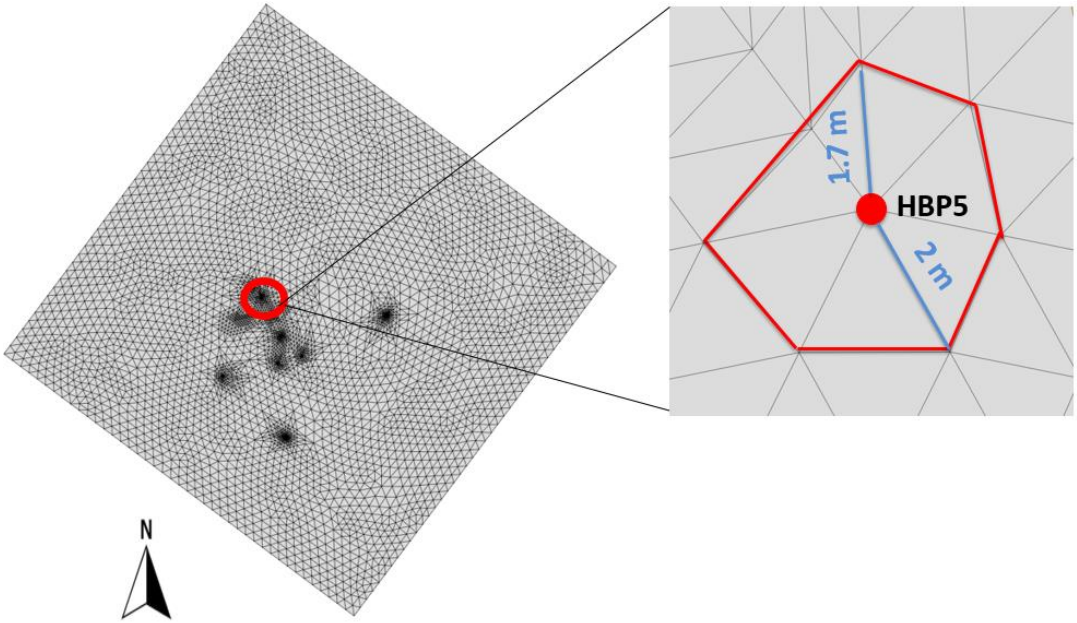

Figure 2-5: Mesh discretization on the domain (on the left). The masked area around HBP5 (in red) used to calculate the subdomain budget (on the right).

The simulated flow rate across the masked area was used to obtain the relative water exchange between the borehole and the HGUs (positive and negative flow rates represent flow into/out of the borehole, respectively). The cross-sectional area for flow during flowmetering is the annular space between the 1 5/8-inch probe and the 6-inch hole assigned to the line element to represent the open borehole at the HBP5 location. An hydraulic aperture of 148 µm was assigned to the line element representing the open borehole in the numerical model, obtained from the mean hydraulic aperture from packer testing reported by Belan (2010) for the Guelph and Gasport Formations and consistent with the range in hydraulic apertures (15-407 um) reported on by Munn (2012). The model performance was evaluated against the measured blended head and flow responses from the flowmeter logs. The goal was to provide a model that reproduces the high-resolution data under a hydrogeological defensible conceptual site model. Then, the model was further examined under various hypothetical scenarios.

3 Results and Discussion

The initial cutout model had three hydrostratigraphic layers in the overburden corresponding to the regional model. The overburden MLSs (shown by yellow points in Figure 2-2:D) were used as preliminary available data to refine the position and thickness of those three units to be locally relevant to this study (Stockford, in progress). MPS4 is one of these MLSs located adjacent to HBP5 (~ 3 m away) and the data from this borehole were used to specifically improve the model representation of the overburden at HBP5 location. The refinement to the overburden layers was made through the correlation of data from MPS4 including natural gamma, lithology, and vertical head and gradient. Figure 3-1: shows the high-resolution data from MPS4 and the boundaries of the refined overburden unit (in red), labeled M1-M3.

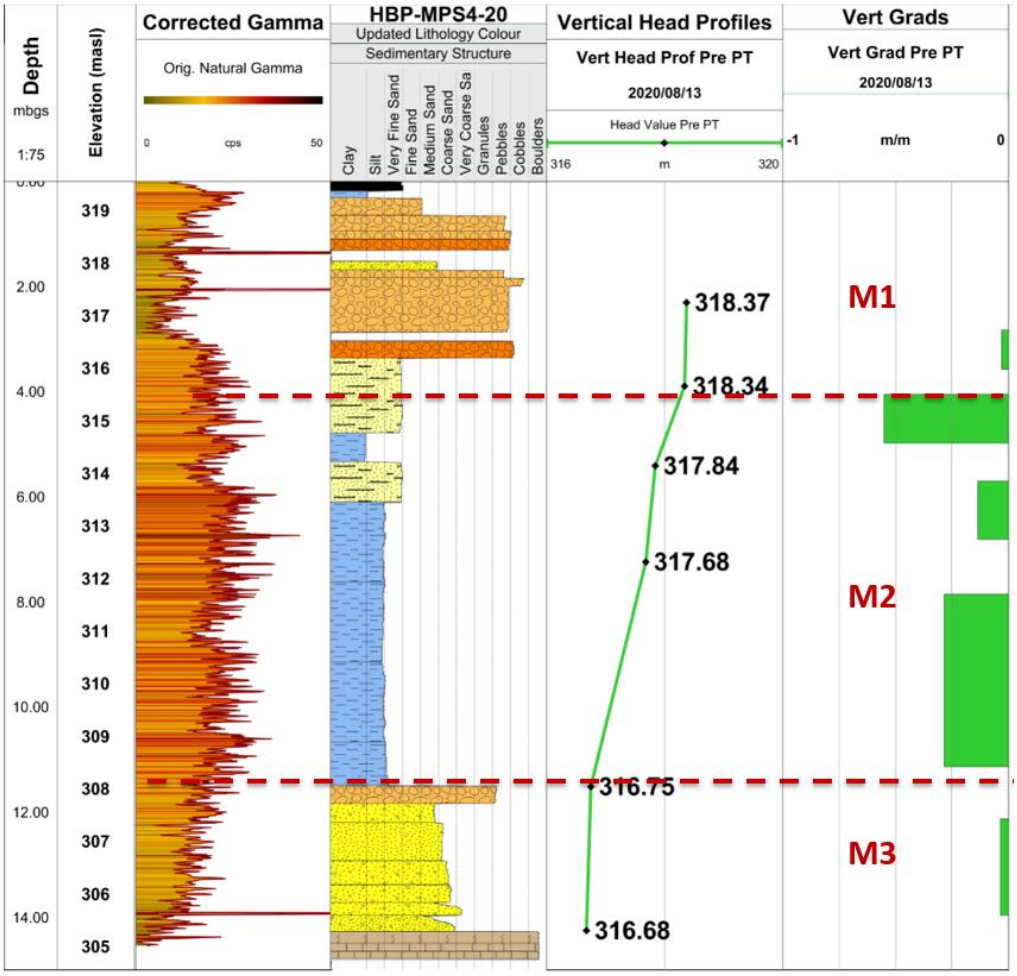

Figure 3-1: High-resolution data from multi-level system well (MPS4) monitoring the overburden.

At HBP5, the continuous core (~85 m deep) from the top of the bedrock (Guelph Formation) to the underlying shale (Cabot Head) provided the foundation for the

identification of lithostratigraphic units. Excellent recovery of 100% on every run was indicative of the competent dolostone. A combination of core data, geophysical logs including natural gamma and ATV, and core photos provided multiple lines of evidence for lithostratigraphic interpretation. Gamma was used to infer changes in lithology and core photos showed matrix color. At the HBP5 location, 11 distinct stratigraphic formations and members were identified within the full stratigraphic sequence in the Silurian dolostone (Brunton and Britnel, 2011). Table 3-1: summarizes the lithostratigraphic units and the properties associated with them.

Table 3-1: Depths of stratigraphic contacts and thicknesses of stratigraphic units at HBP5

Stratigraphy		GS elevation ~323 m asl	
Formation	**Member**	**Top Depth (m bgs)**	**Thickness (m)**
Overburden		0	14.3
Guelph	Wellington	14.27	6.21
Eramosa	Stone Road	20.48	1.62
	Reformatory Quarry	22.1	5.82
	Vinemount	27.91	5.5
Goat Island	Ancaster	33.42	0.48
	Niagara Falls	33.90	3.68
Gasport		37.58	39.35
Irondequoit		76.93	5.18
Rockway		82.11	0.99
Merritton		83.11	1.4
Cabot Head		84.5	0.69

The structural log from the acoustic televiewer contains information about fracture depth, dip direction, and dip angle, essentially providing accurate measurements of fracture orientations. The total number of fractures identified across HBP5 was 274. The fracture network consists of bedding plane fractures (low-angle) and near-vertical joints (high-angle, which looks like a big sine wave). Approximately 95% of fractures across HBP5 were horizontal (dip < 45°) and 5% are near-vertical (dip > 45°).

The hydrophysical logs from straddle packer measurements and flowmeter testing at HBP5 were examined to understand the behavior of the major fractures/zones contributing to the flow into/out of the borehole, and the aquifer transmissivity. The borehole had extreme downward flow between depths of ~ 22 to 39 m bgs (from near the bottom of the Eramosa-Stone Road to the upper Gasport), greater than the logging speed used. The correlation/comparison of hydrophysical logs with ATV, TVP, and the video log as secondary datasets provided supplementary insights into the identification of 20 hydraulically significant fractures intersected by HBP5. There are very subtle differences

in each of these logs; however, within the big picture (i.e. the scope of this study), these subtle differences are not critical since this study only looks into the hydraulically major features. The comprehensive analysis of all the datasets (geological, geophysical and hydrophysical data) resulted in the refinement of the HGU's boundaries across the bedrock. Figure 3-2 shows the positions of major fractures across HBP5 along with the boundaries of the model layers (in red). These features might not all be hydraulically active but they could be the termination of orthogonal fractures that influences the vertical components of gradient.

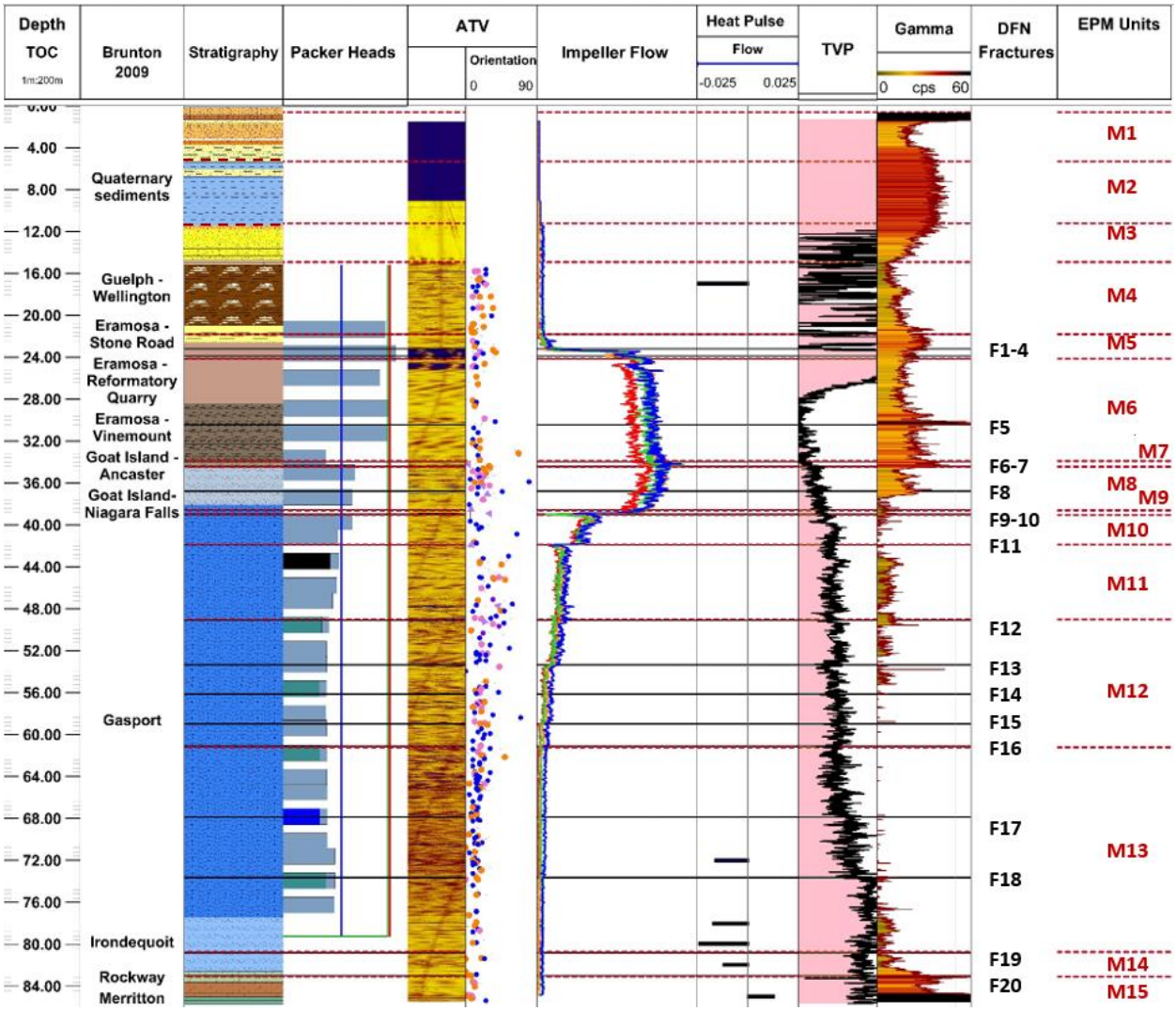

Figure 3-2: Depth-aligned high-resolution datasets from HBP5. Black lines show the positions of hydraulically significant fractures (Fn) and red lines demonstrate the boundaries of the model layers (Mn) while n shows the number (e.g. F1 shows the first major fracture).

On the flowmeter profiles (impeller and heat pulse logs), any changes to the right indicate inflow to the borehole from formations/fractures while any changes to the left show flow

leaving the borehole. Sharp changes are evidence of major transmissive features contributing to a significant amount of water moving into/out of the system while gradual changes are more indicative of several smaller fractures contributing to a small amount of flow in/ out of the borehole.

Moving down the hole, the flow gradually increases when the impeller flow meter passes the first major feature (F1). At 22.9 m bgs, a big spike is seen on the impeller log that is evidence of a highly transmissive fracture (F2) contributing to the majority of flow into the hole. The video log also indicates a large aperture fracture with a very smooth surface that can be interpreted as a strong dissolution enhanced fracture. Gradual increase of flow between 23.6 to 33.7 m bgs is evidence of several smaller fractures across this zone (M6). The whole flow response in the upper portion of the flowmeter profile is dominated by the first four peaks in a row (F1-4) that are the noticeable measure of the increase in “flow into” the borehole. The flow continues to increase gradually and reaches a new maximum at depth of 33.7 m bgs and immediately decreases (goes towards the left side of the impeller log). Analysis of ATV and video log indicates two parallel fractures at this depth (F6 and F7). Excellent correlations between the impeller flow log and the hydraulic head profile from packer measurements provide evidence of a “head loss” occurring across the zone between these two fractures (M7) which is a relatively thin zone (~ 30 cm). The top fracture (F6) has a high head where the water is shunted into that lateral feature, essentially dissipating that energy below it and once the probe passes the bottom fracture (F7) that is in a “low head zone” the flow starts to decrease. These two bedding-parallel transmissive features occur within the Ancaster member of the Goat Island Formation. The zone in between (M7) is a transition zone where the flow profile starts transitioning from inflow to outflow (right to left). Based on the borehole impeller log and the head loss from the packer data, the transition from flow into the borehole to out of the borehole across these two fractures occurs due to a change in hydraulic head and suggests the presence of a thin aquitard within this member. This is consistent with similar bedding parallel features and aquitard properties within the Ancaster member found in other parts of the City (Munn, 2019).

A sudden drop on the flowmeter log from 38.0 to 38.4 m bgs shows that a significant amount of water is leaving the borehole through two parallel fractures with big apertures (F9 and F10). Flow continues to decrease by losing water to the next fractures in the line indicated by small steps on the profile (F11-16) and the trend of the impeller data is fairly flat (steady flow rate) from a depth of 60.6 m bgs (middle Gasport) to the bottom of the hole where the impeller flow data is of poor resolution. Thus, the temperature vector probe (TVP) and heat pulse flow logs were used to provide complementary insights into the identification of other hydraulically important fractures at the lower portion of the borehole. At depth of 67.3 m bgs (F17), for instance, the TVP log captures a nice temperature change that is almost imperceptible in the impeller flow log due to the poor resolution. All

the heat pulse tests indicated downward flow except for the deepest test near the bottom of the hole in the Rockway Formation, which showed a change in direction of flow. This upward water movement indicates that the head below the depth of this test (82.4 m bgs) is higher than the blended head above. This can be explained by the higher head commonly observed in the Cabot Head Formation at the base of the sequence relative to the Gasport Formation (Kennel, 2008; Johnson, 2020; Meyer et al. 2014). The insight from the heat pulse log corroborated by the TVP and ATV logs resulted in the identification of four more hydraulically active fractures (F17-F20) across the bottom of the hole (Figure 3-2). The model layers and the properties associated with them including depth, relative contribution to flow in/out of the borehole, major fractures across the zone, relative head, and lithology are summarized in Table 3-2 (See Appendix A for more details on these fractures).

Table 3-2: The EPM model layers and the properties associated with them

EPM Layer	Depth (m bgs)		Thickness (m)	Flow Regime	Relative Head	Significant fractures	Lithostratigraphy
	Top	Bottom					
M1	0	4.0	4.0				Coarse-grained outwash gravel, sand, Till deposits (sandy/stony silty, sand, etc.)
M2	4.0	11.3	7.3				Clay, sand, silt and Till deposits
M3	11.3	14.3	3.0				Coarse textured gravel, sand deposits
M4	14.3	21.3	7.0	Flow into the borehole	High		Guelph/ Eramosa-SR
M5	21.9	23.6	2.3		Very High	F1-4	Eramosa-SR/RQ
M6	23.6	33.7	10.1		High	F4-6	Eramosa- RQ/V
M7	33.7	33.9	0.2		Very Low	F6-7	Goat Island- A
M8	33.9	38.0	4.1	Flow out of the borehole	Intermediate	F7-9	Goat Island- NF/ Gasport
M9	38.0	38.4	0.4			F9-10	Gasport
M10	38.4	41.4	3.0			F10-11	
M11	41.4	48.7	7.3		Low	F11-12	
M12	48.7	60.6	11.9			F12-16	
M13	60.6	80.7	20.1			F16-19	Gasport/ Irondequoit
M14	80.7	82.4	1.7		Higher than above	F19-20	Irondequoit/ Rockway
M15	82.4	85.5	3.1	Flow into borehole			Rockway, Merriton, Cabot Head

The flow in/out of the borehole (either substantial or less substantial) distributed over a vertical height or compressed into a very narrow interface (e.g., fracture) is driven by the local head differential and the amount of the flow is controlled by conductivity of the discrete features. Head differential is the difference between the depth-discrete ambient

heads in the formations in the surrounding aquifer and the blended head in the open borehole. The blended head is a result of equilibrium in the hole while the local head at each zone can be either higher or lower in the formation and can vary along the borehole. The transmissivity may be depth discrete at interfaces with larger transmissivity or may be distributed over zones with smaller transmissivity. The flowmeter log only notices the features/zones with the right combination of conditions (transmissivity and head differential).

This study began with the development of a smaller “cutout ” model based on the calibrated regional groundwater flow model. To take advantage of the available high-resolution datasets for the Guelph aquifer, model layers were originally informed by 12 bedrock HGUs established from the pre-existing advanced field-based studies (Belan, 2010; Munn, 2012; Munn, 2019; Skinner, 2019; Johnson, 2020). The SCM layers in the overburden were informed by the regional model (3 layers). To tailor this to a site-specific framework representative of the local conditions, the SCM layers (boundaries and thicknesses) were refined through a comprehensive analysis of the high-resolution datasets from HBP5. Figure 3-3: shows the new cutout model layers and compares them with the lithostratigraphic column. It can be inferred that the model EPM boundaries are not necessarily aligned with lithostratigraphy.

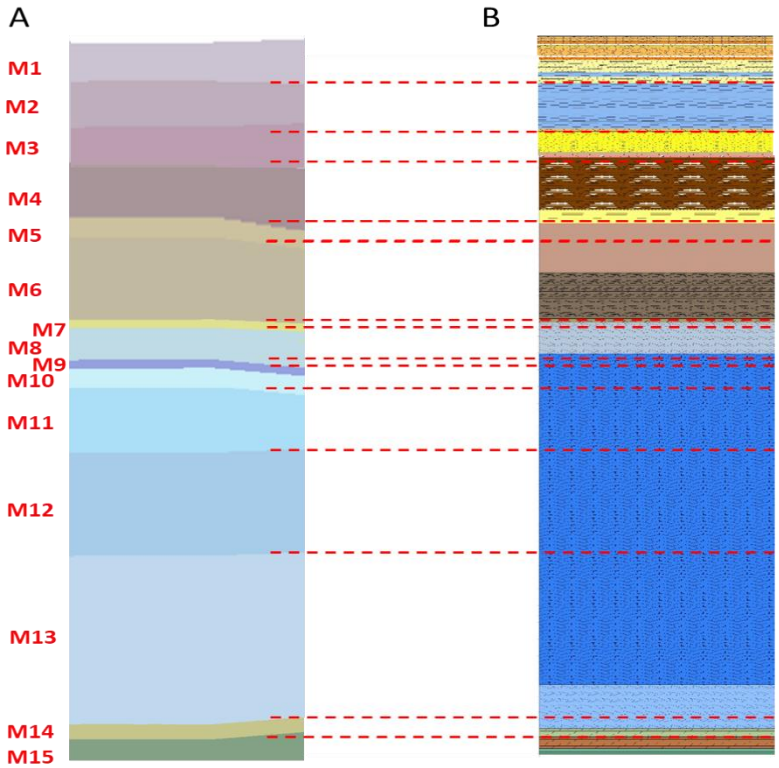

Figure 3-3: (A) the refined model layers. (B) HGU boundaries (in red) on the lithostratigraphy.

3.1 Model Calibration and Sensitivity Analysis

The input hydraulic parameters of the model were calibrated to 40 depth-discrete hydraulic head data points (measured in winter/summer 2020) from the monitoring wells (Figure 2-2:D). The modifications to these parameters were reasonable and within the range supported by the estimated/calibrated values in the Guelph area (Kennel, 2008; Meyer et al. 2014; Matrix Solutions Inc., 2017; Munn, 2019; Skinner, 2019; Johnson, 2020). The calibrated Kh/Kv ratio ranges from 1-100 representing predominantly horizontal groundwater flow within the aquifer. The calibrated recharge rates for the entire domain vary between 5 and 250 mm/y which is within the range of the estimated values for the calibrated regional model (see Appendix D for more details). The modified specified heads were also within the predicted values from the regional potentiometric maps (Appendix D) except for M5 where higher values were assigned to mimic the pressurization/ artesian condition. The calibration performance was evaluated using graphical analysis including a scatter plot, histogram, and statistical parameters. Figure 3-4 illustrates that the EPM model can simulate the high-resolution vertical head data without considerable systematic errors, provideing satisfactory results. The correlation coefficient (R^2) of 0.9, root mean square error (RMSE) of 1.36 m, normalized root mean square error (NRMSE) of 0.004, mean error (ME) of -0.22 m, and mean absolute error (MAE) of 1.10 m were all within the acceptable hydraulic head errors (Levison et al. 2014; Persaud et al. 2020) and the small errors can be explained by the assumptions associated with the EPM approach that does not fully represent a heterogeneous fractured aquifer system. Table 3-3 compares the layers and the calibrated hydraulic parameters of the revised SCM to the regional model (Matrix Solutions Inc., 2017).

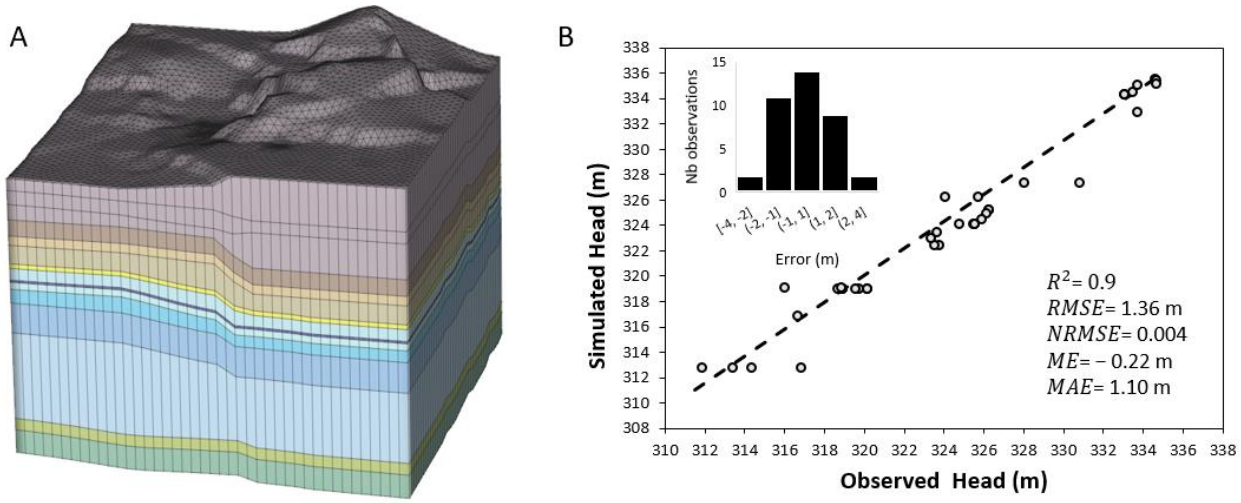

Figure 3-4: A) the revised 3D static SCM, (B) a comparison of measured and simulated heads (40 depth-discrete head points) and associated errors (coefficient of determination (R^2), root mean squared error (RMSE), normalized root mean squared error (NRMSE), mean error (ME), and mean absolute error (MAE); histogram showing the frequency of the mean error.

Table 3-3: Comparison between the calibrated cutout model and the regional model

Cutout Model						Regional Model					
EPM Layer	Stratigraphy	Kx=Ky (m/s)	Kx/Kz Ratio	Recharge (mm/y)	SH (m asl)	EPM Layer	Stratigraphy	Kx=Ky (m/s)	Kx/Kz Ratio	Recharge (mm/y)	SH (m asl)
M1	Sand, Gravel, Clay, Silt, and Till deposits	8E-03-1E-08	1-10	5-250	300-332	1	Gravel, sand, and Till deposits	2.5E-03-1E-06	10-100	5-400	300-332
M2		2E-04-3E-09	10			2		2.5E-04-1E-07	1-10		
M3		9E-03-1E-07	10			3	unconsolidated deposits	2.3E-03-5E-07	1-10		
M4	Guelph, Eramosa-SR	2E-05-1E-09	10			4	Guelph, Eramosa-SR	8E-04-1.5E-07	1-100		
M5	Eramosa-SR,RQ	9E-03-1E-05	1-10		330-340	5	Eramosa-RQ	8E-04-5E-07	1-100		
M6	Eramosa-RQ,VM	9E-04-1E-10	10		300-332	6-8	Eramosa-V	1E-07	100		
M7	Goat Island- An	1E-07	100			9	Goat Island	5E-06-1E-06	1-100		296-326
M8	Goat Island-NF	1E-05-1E-06	1-10		296-324						
M9	Gasport	9E-05-1E-09	1								
M10		2E-05-1E-07	10-100			10	Upper Gasport	5E-05-1E-06	1		
M11		2E-05-4E-06	1			11	Middle Gasport	5E-04-1E-06	1		
M12		6E-05-1E-07	1-100			12	Lower Gasport, Irondequoit, Rockway, Merritton	2E-06-1E-06	1-100		
M13	Gasport, Irondequoit	6E-05-1E-07	1-100			13	Cabot Head	1E-10	100		
M14	Irondequoit, Rockway	1E-06	10								
M15	Rockway, Merritton, Cabot Head	1E-09	100								

The calibrated parameters were modified to perform the relative sensitivity analysis. The sensitive variables were ranked in descending order: K_b, specified head, and recharge, where the most sensitive parameter was bulk hydraulic conductivity. Figure 3-5 demonstrates the relative sensitivity of the heads to changes in the K_b parameter. The other two parameters have different scales of the relative sensitivity and they were not shown on the same plot (see Appendix C). Variations in specified head values affected the calibration results indicating that although these boundaries are located far enough away from HBP5 (~ 4-6 kms away) and other monitoring wells (at least 2.5 kms away), they are still able to influence the head distributions within the domain and therefore, caution must be taken on further predictions/interpretations of the aquifer system. Changes in recharge rates had more impacts on the hydraulic heads in the shallow system than those in the bedrock (see Appendix C).

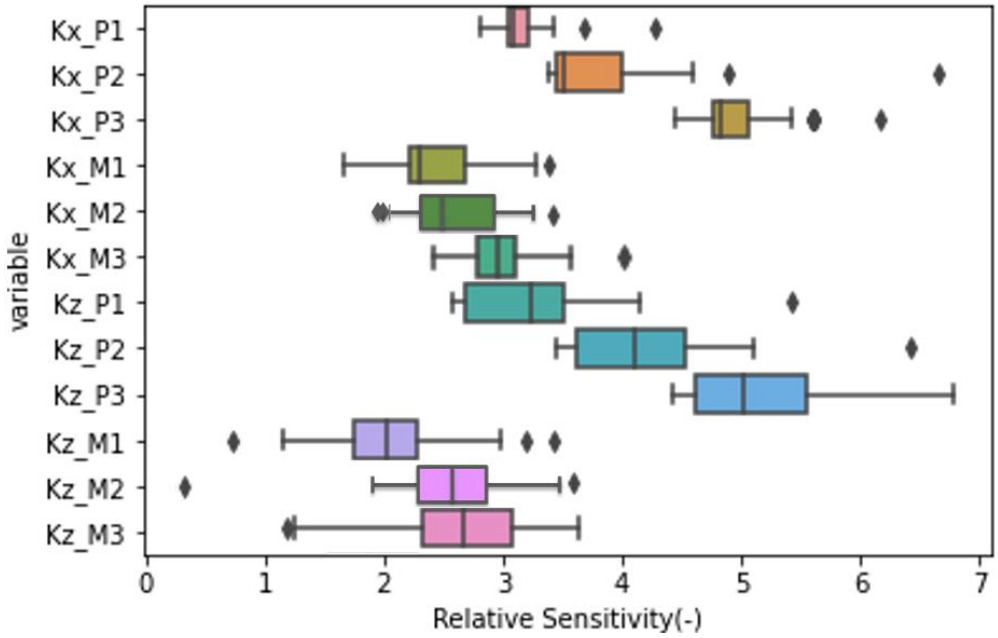

Figure 3-5: Relative sensitivity of hydraulic head points to variations of horizontal/ vertical K_b. For example, Kx +1 on the plot indicates a (positive) one-order of magnitude change in horizontal K_b.

3.2 Model Verification

After calibration, a single borehole (6-in hole) was introduced into the domain at the HBP5 location (see Figure 2-2:D) and the model performance was evaluated against: 1) the blended hydraulic head; and 2) the flow response across the open hole. The open hole interval from the top of the bedrock (Guelph Formation) to the bottom (Cabot Head Formation) was ~85 m, allowing vertical flow along the hole.

The static water level observed at the open borehole (HBP5) is the blended head which is different from the depth-discrete heads measured using straddle packers with 1.5 m monitoring interval. The blended head was measured with a water level tape after the hole was open for a day. A comparison between the simulated blended head and that measured in the field indicated that the simulated blended head was approximately 1 m higher than that measured likely due to assumptions of the EPM approach as well as the Hagen-Poiseulle equation. There are also two pumping wells (shown in Figure 2-2:D) in the area that were not simulated in this model that might temporally impact the field-measured static head value, although this was not investigated explicitly. Figure 3-6 shows the flow distributions under (A) ambient system versus (B) the cross-connected system, illustrating that the blended head is not indicative of the gradient across the borehole. Therefore, using the open hole flow dynamics to represent ambient heads essentially results in misleading information and interpretations about the behavior of the groundwater flow system. This is an important premise for what is occurring in cross-connected systems.

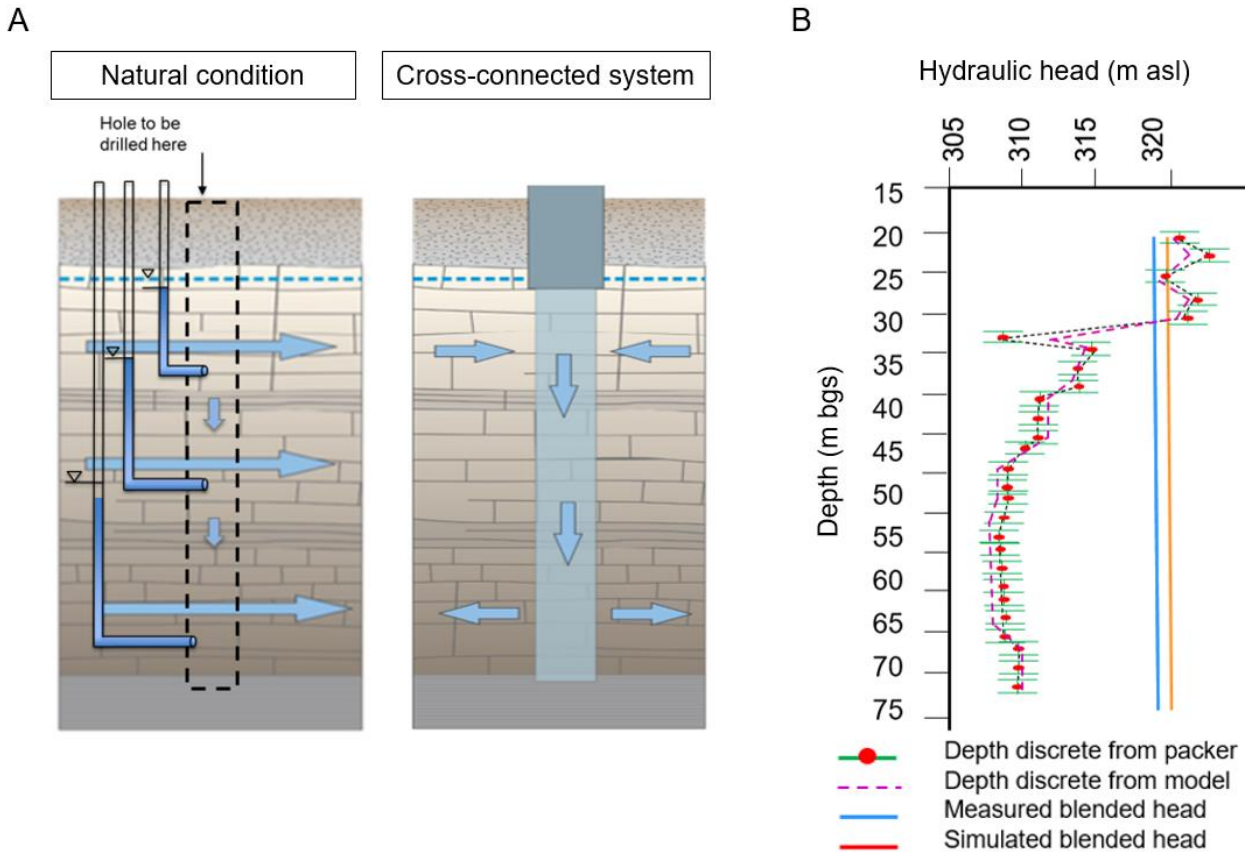

Figure 3-6: (A) Conceptual diagram indicating how the vertical flow in the open well changes the flow distributions as opposed to natural conditions (modified from J Munn). (B) a comparison of the measured and simulated hydraulic heads at HBP5 under open and sealed conditions.

The line element acts as a conduit allowing for vertical flow within the hole and hydraulic cross-connection between the hydrogeologic units. As a result, areally-extensive hydraulic response cones were developed as far away as 6 km from HBP5. The cross-connection relieved the pressure from the pressurized layer (M5) by drawing groundwater from kilometers away, causing drawdown cones on this unit, and releasing it to the deeper units. The pressure propagated down to the deeper units and the main aquifer gets pressurized (higher hydraulic heads creating drawup or injection cones). Figure 3-7 illustrates the hydraulic responses on the pressurized layer (M5) and the main aquifer (M8). The negative and positive water-level changes are indicative of drawdown and draw up cones, respectively. A maximum drawdown of approximately 3 m occurred in HBP5 across M5 extending over the domain. Substantial draw up cones emerged in the potentiometric surface over the main aquifer with a maximum of approximately 11 m in the borehole. Drawdown contours of 0.40 and 0.20 m extended more than 2 and 4 km away from HBP5 on the pressurized layer and draw up contours of 1.2 and 0.7 on the main aquifer extended to more than 2 and 4 km away (Figure 3-7-A.2 and B.2). The results indicated that open borehole cross-connection can significantly alter the natural flow not only in the vicinity of the borehole but also more regionally.

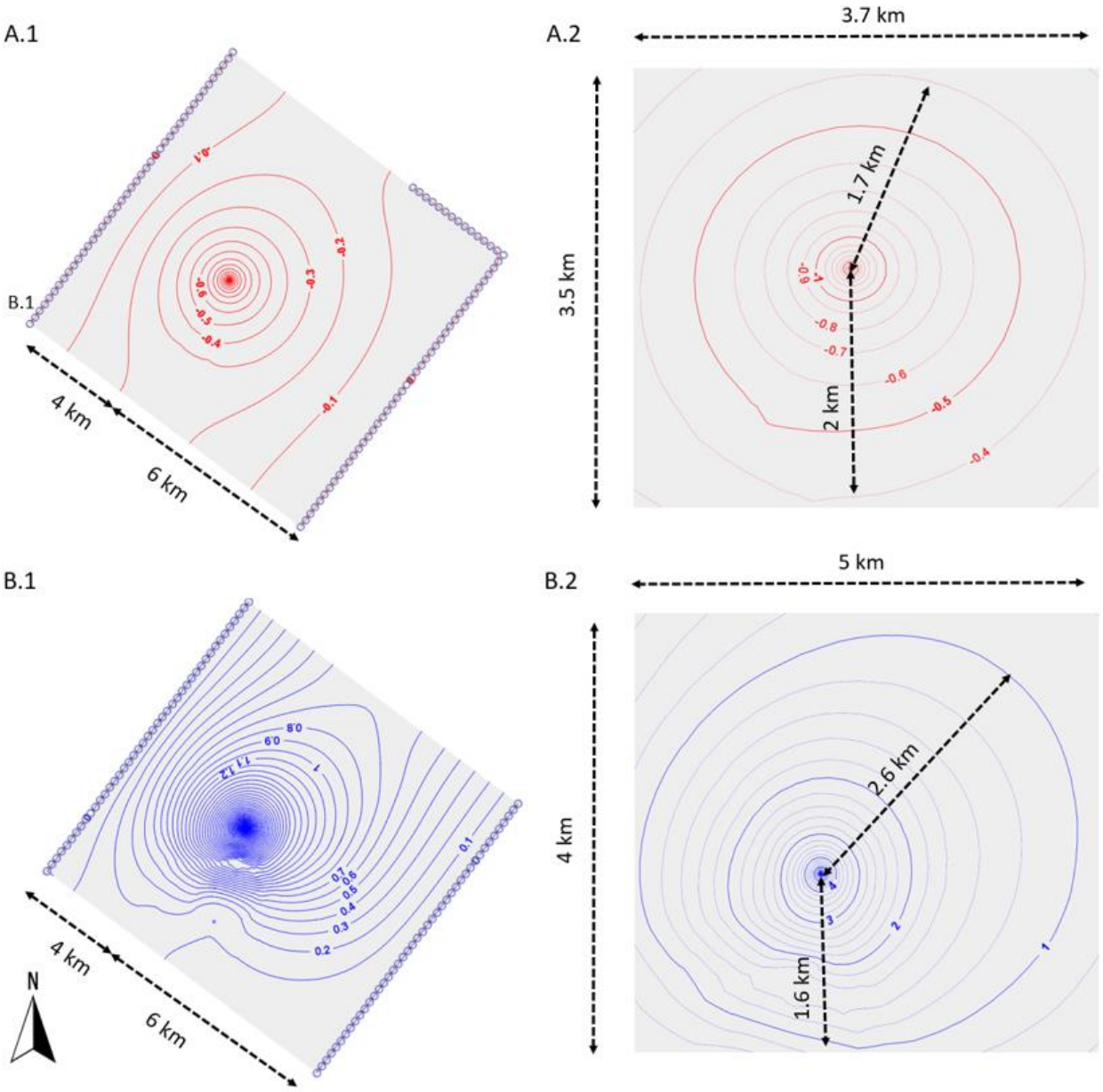

Figure 3-7: (A.1) Simulated drawdown on M5 and (B.1) draw up on the middle Gasport aquifer (M12) extending throughout the domain. (A.2 and B.2) illustrate the asymmetrical hydraulic head responses for the area in the vicinity of HBP5.

Additionally, the measured flow response (from the impeller and heat pulse logs) was qualitatively compared with the simulated response from the EPM model (Figure 3-8). The qualitative analysis of the flow log estimates the relative contribution of each fracture/ zone to the system (whether producing or withdrawing). The simulated response compared well to the actual flow log on a relative magnitude basis and style (i.e. same response pattern and variability along the log is mimicked), showing a reasonable representation of flow variability with depth in and out of the borehole. However,

quantification of this data was more challenging for the portion of the borehole having so much noise due to extreme turbulent conditions. The probe itself does not have polarity which makes it difficult to quantify the vertical velocity in the open borehole (see Appendix B). The patterns of relative changes in flow response have excellent repeatability for the four logs, with the exception of the first log which was conducted immediately after the hole was opened, and likely represents the flow prior to steady-state conditions. The other three logs appear to all be under steady-state conditions indicating that using high-resolution flowmeter data is an effective method to identify the position of important inflow/outflow zones along the borehole. However, for the purposes of this study, these measurements are considered on a normalized relative basis.

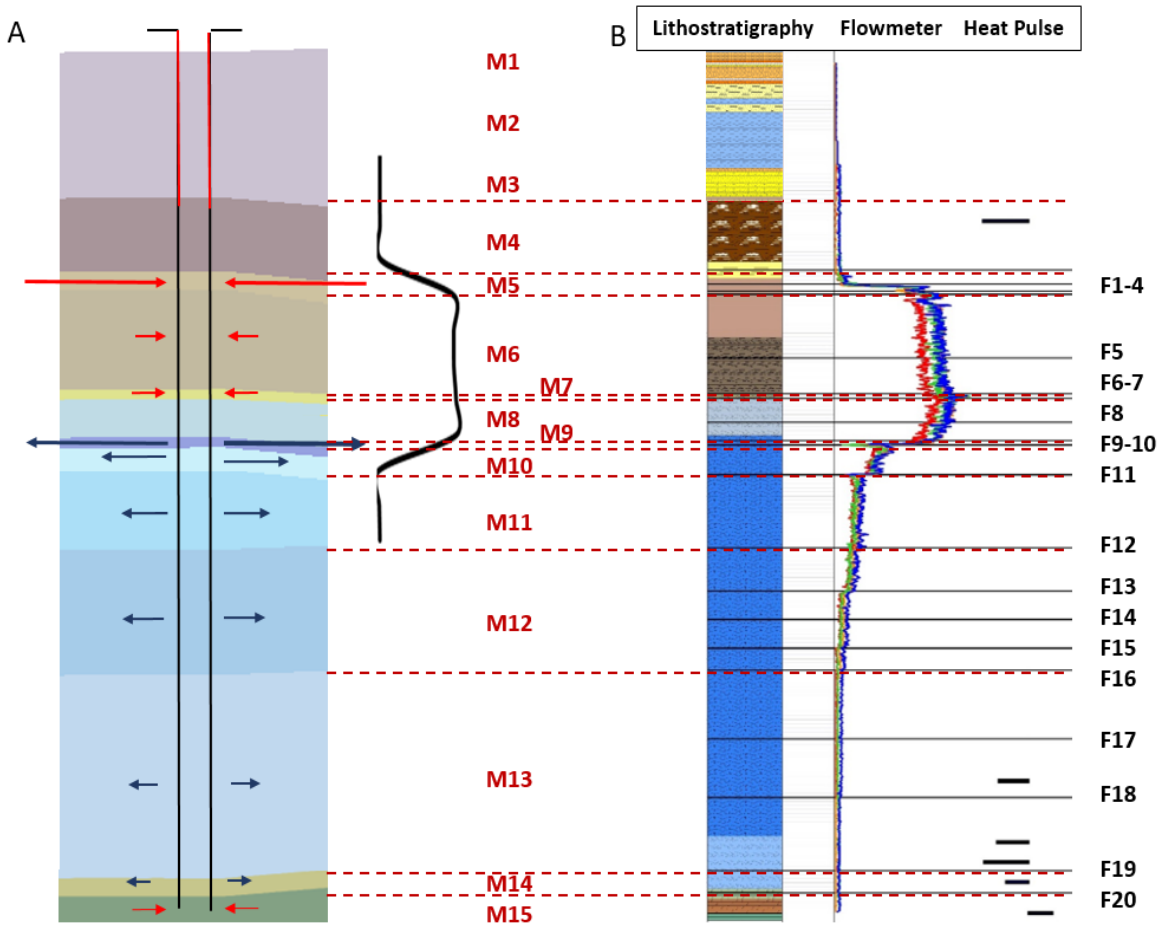

Figure 3-8: (A) The simulated flow response across HBP5. Red and blue arrows represent flow into and flow out of the borehole, respectively. (B) the measured response from the impeller and heat pulse logs indicate that the cross-connected flow is both upward and downward in the hole.

The agreement between the simulated and observed blended head as well as the flow pattern across the hole verified that the refined SCM is a good representation of the system (i.e., HGUs boundaries are likely located in the right positions and the calibrated

parameters are reasonable), decreasing the uncertainty in the non-uniqueness of the calibration process.

3.3 Implications

The model was further examined under a set of hypothetical cross-connection scenarios to: 1) assess the hydraulic head responses; and 2) explore the potential consequences of the cross-connecting wells on the multi-layered aquifer system using forward particle tracking. The base case scenario was defined for “no open borehole” within the entire domain (ambient conditions). Then, the line element was introduced to the bedrock system at the HBP5 location. Scenario A examined the hydraulic responses of the system where the borehole is open across variable well screen length and positions. Scenario B explored the impacts of multi-open overburden boreholes on the system and finally, scenario C is a combined scenario where drilled boreholes are open across the overburden and bedrock. The quantified simulated heads are not shown for scenario C because they were similar to the results from scenarios A and B, and only the result of particle tracking is illustrated herein. The description of scenarios is listed in Table 3-4.

Table 3-4: Description of hypothetical cross-connection scenarios

Scenario	Sub-scenarios	Definition
Base case	----	No open borehole exists
A	A1	HBP5 is open across the bedrock (M4-M15)
	A2	HBP5 is open from the shallow aquifer to the aquitard unit underneath (M4-M7)
	A3	HBP5 is open across the main aquifer (M9-M13)
B	----	Four boreholes are open in the overburden (M1-M3)
C	----	One bedrock borehole (M4-M15) and 3 overburden wells are open (M1-M3)

Scenario A examined a set of sub-scenarios about reducing the screened depth in the bedrock. Table 3-5 summarizes the simulated hydraulic head responses for a few selected layers: the pressurized layer (M5), the Niagara Fall member of Goat Island (M7) behaving as aquitard at this location, and the middle Gasport aquifer (M12). Positive/negative changes in hydraulic heads show the draw ups and drawdowns. The results indicate that reducing the screened (or open hole) depth decreases not only the changes in the water levels (values) but the extent of the response cones within the domain (the response cones become broader when the screened depth is longer). The largest response occurred in scenario A1 where HBP5 was screened across the bedrock. Scenario A2 produced responses consistent with scenario A1; however, the magnitudes are smaller and almost no response was detected across the main aquifer. Scenario A3 shows that if the borehole is only screened across the Gasport aquifer, the hydraulic responses would be so small as to be negligible due to the high transmissivity of the

Gasport Formation and not much head differential across it. The simulated hydraulic head responses in HBP5, in near extent of the borehole, and throughout the domain indicates that open borehole hydraulic cross-connection disturbs the distribution of the flow system locally and even regionally, and this alternation might also impact natural heritage features such as wetlands (discharge areas).

Table 3-5: Simulated hydraulic responses for scenario A. R is the amount of draw up/down at a certain radius from the borehole in meters. X is the distance away from HBP5 (in km).

Scenario	Max R at HBP5	EPM layers	R @ X=0.5 km (m)	R @ X=1 km (m)	R @ X=2 km (m)	R @ X=4 km (m)
A1	11.01@M8 -3.17@M5	M5	-0.80	-0.60	-0.40	-0.20
		M7	3.5	2	1.5	1
		M12	3.3	1.8	1.2	0.7
A2	11.53 @M8 -3.06@ M5	M5	-0.75	-0.50	-0.35	-0.15
		M7	0.15	0.08	0.02	0.01
A3	0.004@M12		---	---	---	---

Scenario (B) examined how the presence of a series of open boreholes in the overburden influences the system responses. It was assumed that the MLSs (MPS1-4) are open in the overburden. Table 3-6 summarizes the simulated hydraulic responses. The results showed the drawdown cones on the top model layer (M1) extending to an area in the vicinity of each well. The negative responses around the boreholes on the top layer (M1) can be attributed to the strong recharge area, downward gradient, and the geology comprised of low permeability materials. The pressure propagated down to the lower unit (M3) resulting in draw up cones. Hydraulic head responses were not considerable at MPS3 and MPS4 (MPS4 is located 3 meters away from HBP5). This can be explained by the artesian condition at HBP5 where the gradient already exists and it is as strong as what it was relative to the scenario where the pressurized unit was cross-connected.

Table 3-6: Simulated hydraulic responses (R) for scenario B (all values are in meters).

Scenario	Max R at MLSs (m)	EPM layers	R @ X=50 (m)	R @ X=100 m (m)	R @ X=200 (m)
MPS1	-0.96 @M1 0.48 @M3	M1	-0.20	-0.10	-0.03
		M3	0.06	0.02	0.01
MPS2	-0.05 @M1 1.08 @M3	M1	-0.02	-0.01	---
		M3	0.16	0.08	0.03
MPS3	-2.60 @M1	M1	-0.10	-0.02	---
		M3	---	---	---

The importance of cross-connection was also illustrated through forward particle tracking. Particle tracking was performed for a few sub-scenarios (A1, A2, B, and C) to illustrate the consequences of cross-connections on flow pathways and the aquifer vulnerability by only evaluating pathways from a streamline/flowline perspective and not the solute transport. The results are illustrated on a selected fence cross-section (south-north direction) crossing HBP5 which is shown in Figure 2-2:C (blue dashed lines). First, the particles (50-100 particles) were released on top of the pressurized layer (M5) for the base case scenario and then from the same starting point but for scenario A1 with a cross-connected flow system. Figure 3-9A illustrates that in the ambient system, particles would follow the natural flow pathways and stay shallow while Figure 3-9B shows how hydraulic cross-connection can bring water from the shallow system to the deeper aquifer that has significant implications for contaminant transport. The vast majority of the particles are flowing through the open borehole. However, some of the particles in the system are migrating upward due to the pressurization that creates an upward flow while at the bottom of the artesian zone, the head is higher than below it which is also driving some particles downward (note that one particle is not equal to one unit of water and it is not volume conservative).

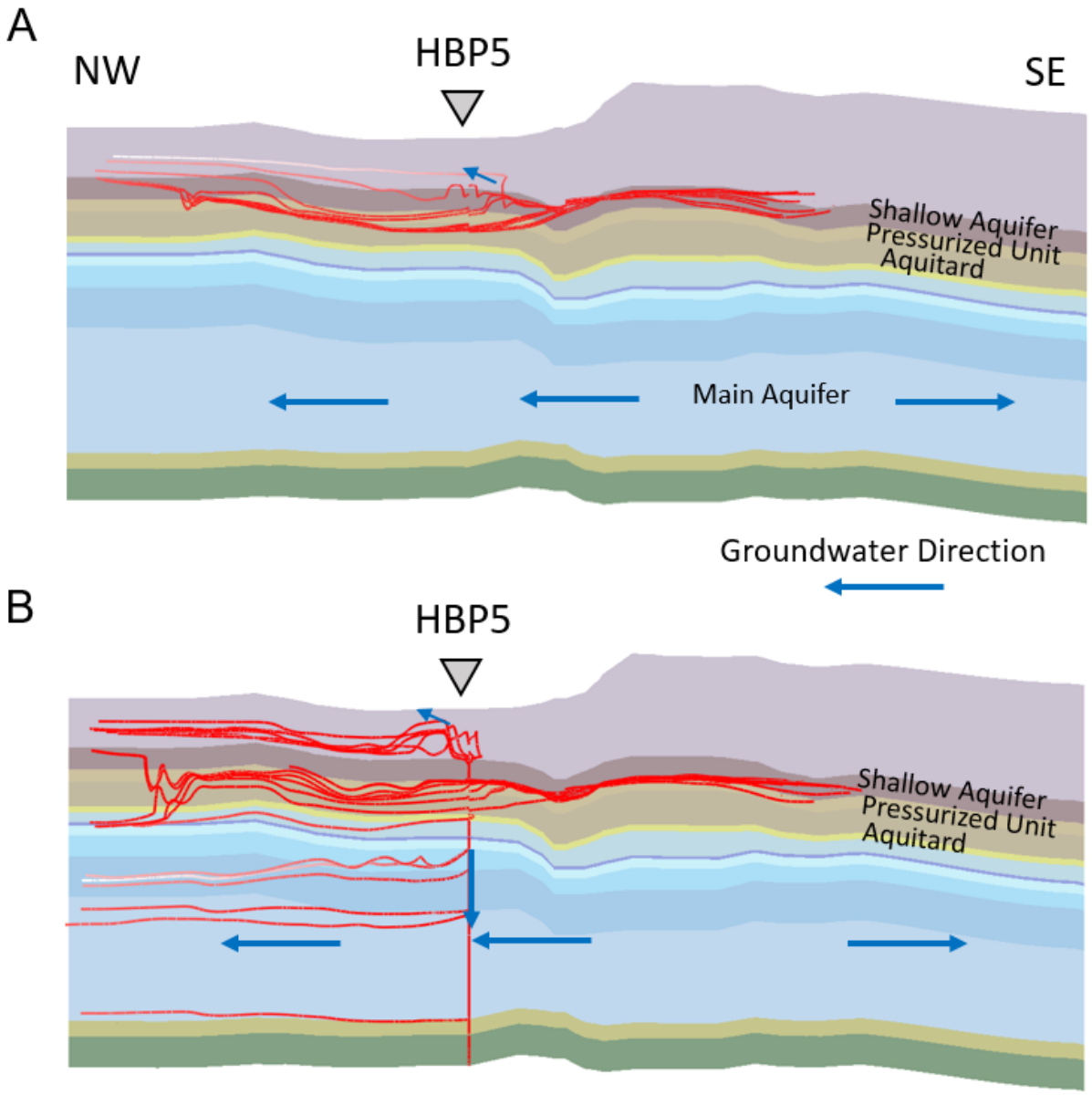

Figure 3-9: The particle pathways under (A) the base case scenario and (B) scenario A1 (the cross-connected scenario). Cross-connection can bring contaminated water that is shallow in the system and re-distributing it deeper to the aquifer.

Particles were released from the same starting point for scenario A2. If the borehole is shortened to only reach the top of the aquitard unit (Ancaster member of Goat Island Formation), disconnecting the upper aquifer from the lower aquifer, that greatly reduces the alteration of the flow field (Figure 3-10). Thus, to prevent cross-connecting pathways and to protect the lower aquifer (i.e. from potential shallow contaminants), it is important that rather than having a long open bedrock borehole, the borehole is cased down deeper, i.e. below the aquitard unit.

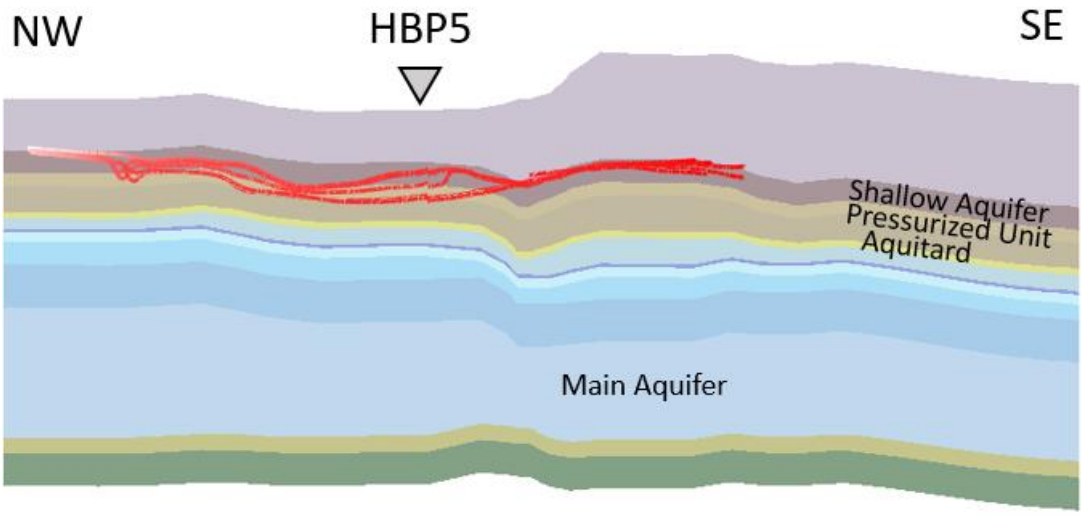

Figure 3-10: The particles pathways for scenario A2 demonstrate that if the aquitard is not cross-connected (due to the shortening of the well screen), the particles stay shallow.

Particle tracking for scenario B with the starting point around the Paris moraine, an area of high recharge (Figure 2-2:D), demonstrated that the particles will remain in the overburden even after introducing cross-connection to the model domain (Figure 3-11). It is shown that if a series of open boreholes exists in the overburden, preferential pathways are introduced for the particles to migrate downward until the artesian effect of the pressurized unit pushes them back up. The head in the pressurized zone is higher than the ground surface, creating upward flow. Thus, the artesian zone underneath the overburden creates a groundwater divide and serves as a hydraulic barrier to the lower units.

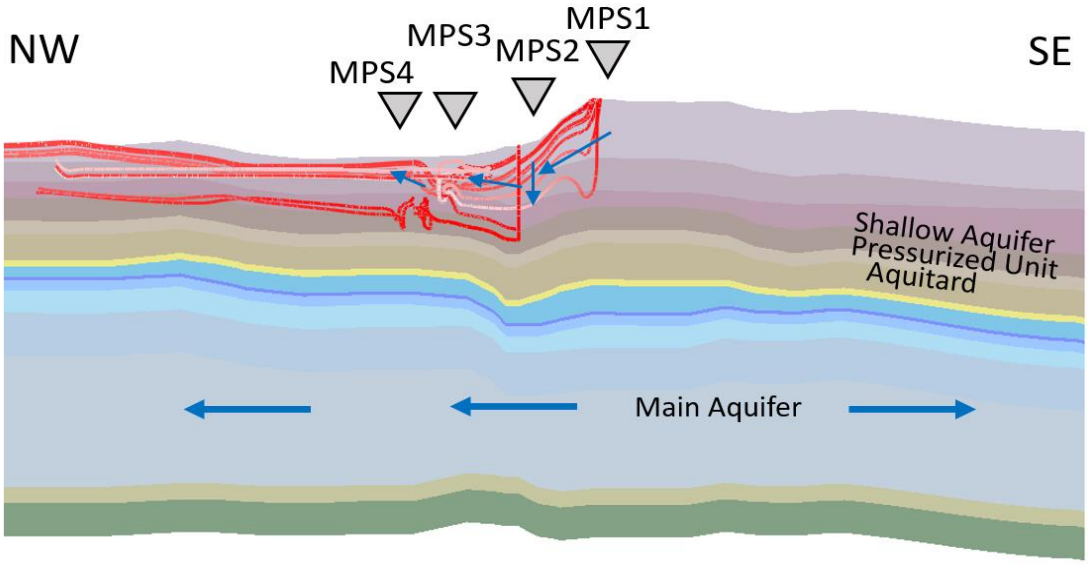

Figure 3-11: The particles pathways for scenario B. Particles can move from one open borehole to the other; however, the upward gradient of the pressurized layer keeps them in the overburden.

Figure 3-12 illustrates the particle tracking for scenario (C). Particles were released from the recharge source (same starting point as scenario B) with a combination of open wells in the system. It is seen that the particles that were held in the overburden due to the efficiency of the artesian barrier, now find their way to the bedrock.

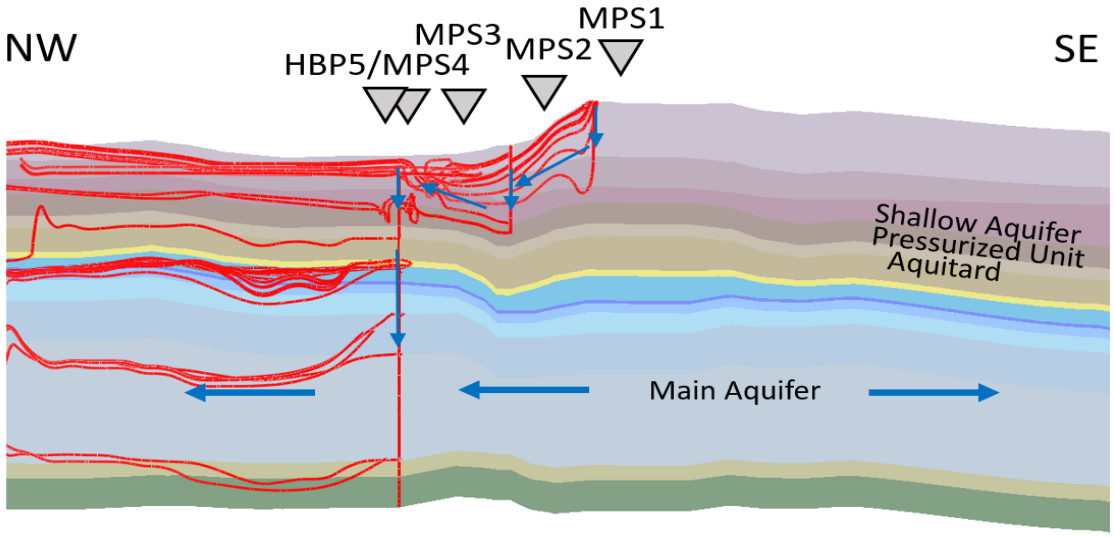

Figure 3-12: The particle pathways for scenario C where a combination of boreholes exists in the overburden and bedrock.

3.4 Limitations

Simulation of cross-connected systems is challenging due to the limitations imposed by the model as well as the site hydrogeologic setting (that is different from site to site). The groundwater FEFLOW model can solve the flow problem mathematically by taking into account information from every single node and flux rates going throughout the model (i.e. it can calculate the flux at the interface intersecting the borehole). However, it is not able to simulate turbulent conditions in open boreholes. The laminar assumptions of the Hagen-Poiseulle equation used in this study have limitations for simulating turbulent conditions in the borehole. This study benefited from using high-resolution data obtained from DFN-M methods. It would be interesting to collect more data from HBP5 using other field methods. However, the extreme turbulence and strong downward gradient in HBP5 made it difficult to obtain other datasets. For instance, it would be very difficult to install a FLUTe liner in such a hole, eliminating the use of DFN-M methods needing such a liner. Furthermore, because of the strong dewatering effect of the shallow zone and influence on a nearby private well, the borehole was not allowed to remain open overnight (e.g.

more flow logs in HBP5). Model predictions could be constrained better if the simulated flow response across the open borehole was quantitatively validated to the field data. The stylized representing HBP5 condition was developed in a steady-state mode using a variety of high-resolution depth discrete datasets because the steady-state assumptions still allow for modeling the hydraulic cross-connection. Transient calibration was not possible as there were not enough transient data available (from the seven boreholes across the domain) during the modeling work.

3.5 Future Work

Transient modeling can be examined in future work to precisely investigate the effects of other cross-connected boreholes and pumping wells across the domain on the flow distribution. The SCM can then be used to produce more realistic hydrogeological models that represent the actual contaminant transport and fate to further address prediction uncertainty about transport pathways, travel time, and residence time. This study showed that the occurrence of open/poorly sealed boreholes influences the groundwater flow system locally and also regionally, and thereby, future studies may also seek to simulate cross-connected systems on a regional scale. The foundation of such models (regional scale) can be built on the concepts learned from this study. The City of Guelph can use the high-resolution datasets available from the advanced monitoring wells across the City to modify/refine the regional model. The strong downward gradient in part of HBP5 made it challenging to do more flow logging and complementary measurement methods (A-DTS, packer testing for transmissivity and aperture estimation, etc), which would be helpful for the quantitative analysis of the flow log, and it would be informative to do this type of investigation in a different hydrogeologic setting. Finally, hydrogeologists, especially modelers would benefit from a powerful tool giving them the option to simulate turbulent conditions in open boreholes that would be useful for accurate simulations/predictions on cross-connected systems. It is recommended that software products consider adding this option into the models.

4 Conclusions

Comprehensive analysis of multiple high-resolution datasets from a borehole is imperative to the identification of hydraulically significant fractures intersected by the borehole and the understanding of the complexity of the flow system. This insight provides a foundation to tailor the SCM details (e.g. the HGU boundaries and the input parameters) to be locally relevant to HBP5 conditions (site-specific). The standard modeling practice is to infer HGUs from lithostratigraphy as opposed to collecting high-resolution data (geological, geophysical, and hydrophysical logs) to inform conceptual model layers. This study showed that the HGU-based model layers do not perfectly correspond with the lithostratigraphy surrounding the HBP5 location and the complexity of flow redistributions (varying amounts of flow and zones of influence occur with discrete depth intervals, some hydrologic units are thick and some are very thin or discrete freatures). The model allowing for an improved understanding of groundwater flow throughout the research domain showed excellent comparison to the actual field data. Although the simulated flow response compares well to the actual flow log on a relative magnitude basis, quantification of these data was more challenging due to the strong vertical gradient across a portion of HBP5.

The head in open boreholes is blended which must be kept in mind when it is used to represent ambient conditions. It is blended due to a non-unique combination of conditions due to depth-discrete transmissivity and hydraulic heads in fractured hydrologic units with varying thickness in the borehole unless high resolution field measurements are made to constrain the distribution of hydraulic head and transmissivities. This study shows reasonably well, although imperfectly due to artesian flow conditions limiting availability of a complete dataset, the ability to represent the characteristics of cross-connected flow. Cross-connection alters natural flow and head conditions locally and even regionally leading to the appearance of hydraulic responses (either drawdowns or draw ups) on different HGUs depending on the hydrogeology of the unit. The flow distributions within a cross-connected fracture network lead to erroneous estimation of hydraulic conditions, misleading interpretations, or limitations of data obtained from the cross-connected wells for management decisions. Different fractures contribute different amounts to the flow system and the amount of flow distributed over a zone or in a fracture is the function of the change in magnitude of the conductivity and/or local head differential.

Cross-connected flow is both upward and downward in the hole. Hydraulic cross-connection can also cause vertical flow of potentially contaminated groundwater in the borehole. It can bring water from the shallow system into the deeper aquifer that otherwise discharges elsewhere which has significant implications for contaminant transport pathways and deeper, semi-confined, or confined aquifer vulnerability. To protect the lower aquifers within a multi-layered variable permeability system where flow lines and fluxes are influenced by low permeable layers, it is important that rather than having a

long open bedrock borehole, consideration must be made for well designs to isolate specific zones within HGUs and avoid crossing them. This results in varying flow trajectories and fluxes to existing receptors (discharge locations, etc.), and creates pathways for potential contaminant transport affecting water quality in the deeper system (e.g. reducing transport times, reaction mechanisms, etc.). Therefore, casing a well through shallower units prevents cross-connection across the deeper units. Another finding specific to this study is that if the artesian zone underneath the shallow aquifer is not cross-connected, it serves as a groundwater flow divide and serves as a natural hydraulic barrier providing complete (or perfect) protection to the lower units. Using long, open boreholes is a common practice especially in fractured bedrock systems. Although the profession has been aware of this condition and its potentially lasting consequences it has not resulted in a change in practice; like many things in this world the time has arrived to adjust and make this important change for water source protection.

5 References

Arnaud, E., McGill, M., Trapp, A., & Smith, J. E. (2018). Subsurface heterogeneity in the geological and hydraulic properties of the hummocky Paris Moraine, Guelph, Ontario. *Canadian Journal of Earth Sciences*, *55*(7), 768–785.

Bear, J., 1993. Modelling flow and contaminant transport in fractured rocks. In: Bear, J., Tsang, C.F., de Marisly, G. (Eds.), Flow and Contaminant Transport in Fractured Media. Academic Press, San Diego, CA, pp. 1–37.

Belan, K. (2010). *Characterizing a Fractured Rock Aquifer With Hydraulic Testing At a Contaminated*. University of Guelph.

Berkowitz, B., Bear, J., & Braester, C. (1988). Continuum models for contaminant transport in fractured porous formations. *Water Resources Research*, *24*(8), 1225– 1236. https://doi.org/10.1029/WR024i008p01225

Brassington FC (1992) Measurements of head variations within observation boreholes and their implications for groundwater monitoring. Water Environ J 6.3(1992):91–100

Brunton, F. (2008). Preliminary revisions to the Early Silurian stratigraphy of Niagara Escarpment: Integration of sequence stratigraphy, sedimentology and hydrogeology to delineate hydrogeologic units. Ontario Geological Survey, Open File Report 6226. Summary of Field Work and Other Activities, pages 31–1 – 31–18.

Brunton, F. (2009). Update of Revisions to the Early Silurian Stratigraphy of the Niagara Escarpment: Integration of Sequence Stratigraphy, Sedimentology and Hydrogeology to Delineate Hydrogeologic Units. Ontario Geological Survey, Open File Report 6240. Summary of Field Work and Other Activities, pages 25–1 to 25–20.

Brunton, F. R., & Brintnell, C. (2011). Final update of Early Silurian Stratigraphy of the Niagara Escarpment and correlation with subsurface units across southwestern ontario and the great lakes basin. Summary of Field Work and Other Activities, 6270, 30–130.

Carneiro, J. F. (2005). A study on new approaches for delineating groundwater protection zones in fractured-rock aquifers. University of London.

Chapman, Steven W., Parker, B. L., Cherry, J. A., McDonald, S. D., Goldstein, K. J., Frederick, J. J., et al. (2013). Combined MODFLOW-FRACTRAN application to assess chlorinated solvent transport and remediation in fractured sedimentary rock. *Remediation Journal*, *23*(3), 7–35.

Chapman, S W, Parker, B. L., Cherry, J. A., Martin, P., Abbey, D., & McDonald, S. D. (2014). Combined EPM-DFN modeling approach for plumes in sedimentary bedrock aquifers. In *DFNE-International Conference on Discrete Fracture Network Engineering*.

Church, P. E., & Granato, G. E. (1996). Bias in ground‐water data caused by well‐bore flow in long‐screen wells. *Groundwater*, *34*(2), 262–273.

Coleman, T. I., Parker, B. L., Maldaner, C. H., & Mondanos, M. J. (2015). Groundwater flow characterization in a fractured bedrock aquifer using active DTS tests in sealed boreholes. *Journal of Hydrology*, *528*, 449–462.

Dewar, H., & Soulard, F. (2010). Human Activity and the Environment: Freshwater Supply and Demand in Canada-2010. *Statistics Canada: Ottawa, ON, Canada*.

Diersch, H.-J. G. (2013). *FEFLOW: finite element modeling of flow, mass and heat transport in porous and fractured media*. Springer Science & Business Media.

Fomenko A (2015) An Integrated Lithostratigraphic and Geomechanical Conceptualization of Dense Fracture Networks in a Shallow Paleozoic Dolostone By Andrey Fomenko Presented to The University of Guelph In partial fulfilment of requirements For the degree Master of Applied. University of Guelph

Frind, E. O., & Molson, J. W. (2018). Issues and Options in the Delineation of Well Capture Zones under Uncertainty. *Groundwater*, *56*(3), 366–376.

Guerin, F. P. M., & Billaux, D. M. (1994). On the relationship between connectivity and the continuum approximation in fracture-flow and transport modelling. *Applied Hydrogeology*, *2*(3), 24–31.

Hess AE (1986) Identifying hydraulically conductive fractures with a slow-velocity borehole flowmeter. Can Geotech J 23(1):69–78

Hommersen, J. (2020). *Assessing the Hydrogeological Properties Influencing Nitrate Distribution in a Shallow Unconfined Dolostone Aquifer and Supply Well Vulnerability*. University of Guelph.

Johnson, K. (2020). *High-Resolution Dynamic Pore Pressure Monitoring to Determine Hydraulic Parameters in a Multi-Layered Bedrock System for Improved Aquifer Vulnerability Assessment and Monitoring by*. University of Guelph.

Johnson, M.D., Armstrong, D.K., Sanford, B.V., Telford, P.G., and Rutka, M.A.1992. Paleozoic and Mesozoic geology of Ontario. *In* Geology of Ontario. *Edited by* P.C. Thurston, H.R. Williams, R.H. Sutcliffe, and G.M. Stout. Special, **4**(2),Ontario Geologic Survey, Toronto, pp. 907–1008.

Keller, C. E., Cherry, J. A., and Parker, B. L. (2014). New method for continuous transmissivity profiling in fractured rock. Groundwater, 52(3):352–367.

Kennel JR (2008) Advances in Rock Core VOC Analyses for High Resolution Characterization of Chlorinated Solvent Contamination in a Dolostone Aquifer. University of Waterloo.

Keller, C. (2017). A New Rapid Method for Measuring the Vertical Head Profile. *Groundwater*, *55*(2), 244-254.

Levison, J, Larocque, M., Fournier, V., Gagné, S., Pellerin, S., & Ouellet, M. A. (2014). Dynamics of a headwater system and peatland under current conditions and with climate change. *Hydrological Processes*, *28*(17), 4808–4822.

Maldaner, C. H., Munn, J. D., Coleman, T. I., Molson, J. W., & Parker, B. L. (2019). Groundwater flow quantification in fractured rock boreholes using active distributed temperature sensing under natural gradient conditions. *Water Resources Research*, *55*(4), 3285–3306.

Matrix Solutions Inc. (2017a) City of Guelph and Township of Guelph/Eramosa Tier Three Water Budget and Local Area Risk Assessment.

Matrix Solutions Inc. (2017b) City of Guelph and Township of Guelph/Eramosa Tier Three Water Budget and Local Area Risk Assessment.

McCuen, R. H. (1973). The role of sensitivity analysis in hydrologic modeling. *Journal of Hydrology*, *18*(1), 37–53.

Meyer, J. R., Parker, B. L., & Cherry, J. A. (2008). Detailed hydraulic head profiles as essential data for defining hydrogeologic units in layered fractured sedimentary rock. *Environmental Geology*, *56*(1), 27–44.

Meyer, J. R., Parker, B. L., and Cherry, J. A. (2014). Characteristics of high resolution hydraulic head profiles and vertical gradients in fractured sedimentary rocks. Journal of Hydrology, 517:493–507.

Meyer, J. R., Parker, B. L., Arnaud, E., and Runkel, A. C. (2016). Combining high resolution vertical gradients and sequence stratigraphy to delineate hydrogeologic units for a contaminated sedimentary rock aquifer system. Journal of Hydrology, 534:505–523.

Moeck, C., Molson, J., & Schirmer, M. (2020). Pathline density distributions in a Null‐Space Monte Carlo approach to assess groundwater pathways. *Groundwater*, *58*(2), 189–207.

Mount Sopris Instruments, The Continuous Spinner Flowmeter: A Velocity Measuring Instrument, from the FLP-2492/KLP-4492 Impeller Flowmeter Manual.

Munn, J. D. (2012). *High-resolution discrete fracture network characterization using inclined coreholes in a Silurian dolostone aquifer in Guelph, Ontario*. *Thesis*. University of Guelph.

Munn JD (2019) Measuring groundwater flow system variability in a fractured carbonate aquifer using fibre optic distributed temperature sensing. 234.

Munn, J. D., Maldaner, C. H., Coleman, T. I., & Parker, B. L. (2020). Measuring Fracture Flow Changes in a Bedrock Aquifer Due to Open Hole and Pumped Conditions Using Active Distributed Temperature Sensing. *Water Resources Research*, *56*(10), e2020WR027229.

Myers, T. (2012). Potential contaminant pathways from hydraulically fractured shale to aquifers. *Groundwater*, *50*(6), 872–882.

Neuman, S. P. (2005). Trends, prospects and challenges in quantifying flow and transport through fractured rocks. *Hydrogeology Journal*,*13*(1), 124–147.

Paillet FL (1998) Flow modeling and permeability estimation using borehole flow logs in heterogeneous fractured formations. Water Resour Rec 34(5):997–1010

Paillet FL (2000) A field technique for estimating aquifer parameters using flow log data. Ground Water 38(4):510–521

Paillet FL (2001) Hydraulic head applications of flow logs in the study of heterogeneous aquifers. Ground Water 39(5):667–675

Parker, B. L., Cherry, J. A., & Chapman, S. W. (2012). Discrete fracture network approach for studying contamination in fractured rock. *AQUA Mundi*, *3*(2), 101–116.

Parker, B. L., Bairos, K., Maldaner, C. H., Chapman, S. W., Turner, C. M., Burns, L. S., Plett, J., Carter, R., and Cherry, J. A. (2018). Metolachlor dense non-aqueous phase liquid source conditions and plume attenuation in a dolostone water supply aquifer. Geological Society, London, Special Publications, 479:SP479.9.

Pehme PE, Parker BL, Cherry JA, Molson JW, Greenhouse JP (2013). Enhanced detection of hydraulically active fractures by temperature profiling in lined heated bedrock boreholes. J Hydrol 484:1–15

Pehme, P., Parker, B. L., Cherry, J. A., & Blohm, D. (2014). Detailed measurement of the magnitude and orientation of thermal gradients in lined boreholes for characterizing groundwater flow in fractured rock. *Journal of Hydrology*, *513*, 101–114.

Persaud, E., Levison, J., MacRitchie, S., Berg, S. J., Erler, A. R., Parker, B., & Sudicky, E. (2020). Integrated modelling to assess climate change impacts on groundwater and

surface water in the Great Lakes Basin using diverse climate forcing. *Journal of Hydrology*, *584*, 124682.

Pierce, A. A., Chapman, S. W., Zimmerman, L. K., Hurley, J. C., Aravena, R., Cherry, J.A., & Parker, B. L. (2018). DFN-M field characterization of sandstone for a processbased site conceptual model and numerical simulations of TCE transport with degradation. *Journal of contaminant hydrology*, *212*, 96-114.

Pilato, T. (2021). Exploring the Statistical Method of Moments for Solute Transport in Fractured Porous Rock Aquifers: Bridging the Gap between Local and Regional Scales. University of Guelph.

Pitrak M, Mares S,KobrM(2007) Asimple borehole dilution technique in measuring horizontal ground water flow. Groundwater 45(1):89–92

Poeter, E. P. and Gaylord, D. R. (1990). Influence of Aquifer Heterogenity on Contaminant Transport at Hanford Site. Ground Water, 28(6).

Poulsen, D. L., Cook, P. G., Simmons, C. T., McCallum, J. L., & Dogramaci, S. (2019). Effects of intraborehole flow on purging and sampling long_screened or open wells. *Groundwater*, *57*(2), 269–278.

Price, M., & Williams, A. (1993). The Influence of Unlined Boreholes on Groundwater Chemistry: A Comparative Study Using Pore-Water Extraction and Packer Sampling. *Water and Environment Journal*, *7*(6), 651–659.

Province of Ontario. (2006). *Clean Water Act*. Queen's Printer of Ontario.

Quinn, P. M., Parker, B. L., & Cherry, J. A. (2011). Using constant head step tests to determine hydraulic apertures in fractured rock. Journal of contaminant hydrology, 126(1-2), 85-99.

Quinn, P., Cherry, J. A., and Parker, B. L. (2012). Hydraulic testing using a versatile straddle packer system for improved transmissivity estimation in fractured-rock boreholes. Hydrogeology Journal, 20(8):1529–1547.

Quinn, P., Parker, B. L., & Cherry, J. A. (2016). Blended head analyses to reduce uncertainty in packer testing in fractured-rock boreholes. *Hydrogeology Journal*, *24*(1), 59-77.

Reilly, T. E., Franke, O. L., & Bennett, G. D. (1989). Bias in Groundwater Samples Caused by Wellbore Flow. *Journal of Hydraulic Engineering*, *115*(2), 270–276.

Shapiro, A. M. (2002). Cautions and suggestions for geochemical sampling in fractured rock. *GroundWater Monitoring & Remediation*, *22*(3), 151–164.

Singer, S. N., Cheng, C. K., & Scafe, M. G. (2003). *The hydrogeology of southern Ontario*. Environmental Monitoring and Reporting Branch, Ministry of the Environment.

Skinner, C. (2019). *High-Resolution Hydrogeological Characterization of a Fractured Dolostone Municipal Supply Aquifer to Create a Refined 3-D Conceptual Site Model with Hydrogeologic Units*. University of Guelph.

Sokol, D. (1963). Position and fluctuations of water level in wells perforated in more than one aquifer. *Journal of Geophysical Research*, *68*(4), 1079–1080.

Statistics Canada, Environment and Natural Resources, historical data (1976-1979). Retrieved from: https://climate.weather.gc.ca/historical_data/search_historic_data

Steelman, C. M., Arnaud, E., Pehme, P., & Parker, B. L. (2017). Geophysical, geological, and hydrogeological characterization of a tributary buried bedrock valley in southern Ontario. *Canadian Journal of Earth Sciences*, *55*(7), 641–658.

Sterling, S. N., Parker, B. L., Cherry, J. A., Williams, J. H., Lane, J. W., & Haeni, F. P. (2005). Vertical cross contamination of trichloroethylene in a borehole in fractured sandstone. *Ground Water*, *43*(4), 557–573.

Taylor, B., de Loe, R., Kreutzwiser, R., & Bjornlund, H. (2009). Local groundwater management studies in Ontario, Canada: A case for retaining a role for the state in community-based water research. *Australasian Journal of Water Resources*, *13*(1), 69–80.

Tsang, C_F, Hufschmied P, Hale F (1990) Determination of fracture inflow parameters with a borehole fluid conductivity logging method. Water Resour Res 26(4):561–578

Williams JH, Conger RW(1990) Preliminary delineation of contaminated water_bearing fractures intersected by open_hole bedrock wells. Ground Water Monitor Remed 10(4):118–126

Wilson, J. T., Mandell, W. A., Paillet, F. L., Bayless, E. R., Hanson, R. T., Kearl, P. M., et al. (2001). Evaluation of Borehole Flowmeters Used to Measure Horizontal GroundWater Flow in Limestones of Indiana, Kentucky, and Tennessee, 1999. *Water Resources Investigations Report. United States Geological Survey*, (4139), 144.

A Appendix A: Timeline for DFN-M techniques for HBP5

Table A-1 summarized the timeline for high-resolution DFN-M techniques applied in HBP5 field.

Table A-1: Timeline for the high resolution DFN-M field techniques applied in HBP5

Tool	Date	Task description	Equipment information	Reference	Personnel
Drilling	2019-11-22 to 2019-11-27	A large-diameter (6.625" borehole) Geobor-SG wireline drilling method for lithology,…	Hired from Aardvark Drilling Inc. Model: Eric Deba Top depth: 45.20 ft bgs Bot depth: 279.80 ft bgs	Skinner, 2019	Chrystyn Skinner
Four packer head profile	2020-01-29 to 2020-02-03	Collect the head profile with UoG packer testing equipment	Company name: RST instruments Packer model: 1-85 Deflated length: 40 in Inflated length: 37.5 in Max confined pressure: 375 psi	Quinn et al. 2012	Patryk Quinn
Impeller flowmeter	2020-06-25	Continuously measures large vertical flow in a borehole	Model: FLP-2492/KLP-4492	Piallet 1998 Mount Sopris manual	Pete Pehme
Heat pulse flowmeter	2020-06-25	Measures small vertical flow at specific depths	Model: HPF-2293 Serial No: 3359	Székely, F. & Galsa, A. (2006)	Pete Pehme
Temperature profile	2019-12-04	To measure both the temperature and the characteristics of the thermal gradient.	Model: BTM-04 Serial No: 50923	Pehme et al. 2014	Ryan Kroeker
Gamma	2019-12-04	Measures clay content that implies low permeability or lithology	Model: 2PGA Serial No: 4885	ALT/Mount Sopris manual	Ryan Kroeker
ATV	2019-12-04	Acoustic image of borehole wall identifying fractures with dip and azimuth	Model: abi-40 Serial no: 102602	Alt/mount Sopris manual	Ryan kroeker
Video logging	2020-07-15	Video logged hole	Model: Rcam-100 Serial No: 527		Pat Quinn & Ryan Kroeker

B Appendix B: Hydraulically important fractures across HBP5

The properties associated with the 20 hydraulically significant features across HBP5 are summarized in Table B-1.The indicators are those data mostly used to identify each major fracture.

Table B-1: Hydraulically significant fractures inferred from the HBP5 interpretation

Major fractures	Depth (m bgs)	Flow Regime	Flow Direction	Relative Head (to blended head)	Lithostratigraphy	Indicators			
						Impeller	Heat Pulse	ATV	TVP
F1	21.90	Flow into the borehole	Downward	High	Eramosa-SR	x		x	
F2	22.87		Strong downward flow	Very High	Eramosa-RQ	x		x	
F3	23.31			High	Eramosa-RQ	x		x	
F4	23.61				Eramosa-RQ	x		x	
F5	29.65				Eramosa-V	x		x	x
F6	33.67				Goat Island- A	x		x	x
F7	33.93	Flow out of the borehole		Very Low	Goat Island- A	x		x	x
F8	36.53			Intermediate	Goat Island- NF	x		x	x
F9	38.01				Gasport	x		x	x
F10	38.44					x		x	x
F11	41.42		Downward	Low		x		x	
F12	48.69					x		x	
F13	52.99					x		x	x
F14	55.56					x		x	
F15	58.46					x		x	
F16	60.63					x		x	
F17	67.36						x	x	x
F18	73.14						x	x	x
F19	80.76				Irondequoit		x	x	x
F20	82.45	Flow in	Upward	Higher than above	Rockway		x	x	x

C Appendix C: Quantification of the flow log and challenges

The information presented in this section is provided by Dr. P. Quinn and F. Vahedian.

Flowmeter testing in HBD-MPD5-19 was conducted on the morning of June 25th, 2020. The work was completed in a narrow time window immediately after a packer was removed. The entire hole was examined with the FLP-2492/KLP-4492 Impeller Flowmeter and the lower and upper portions with the HFP-2293 – Heat Pulse Flowmeter; both probes are manufactured by Mount Sopris instruments of Denver, Colorado. The impeller flowmeter measures the velocity of water movement in the open hole relative to the probe (either stationary or moving) based on the spin of an impeller which generates a series of electrical pulses that are transmitted to the surface allowing the measurement of the number of revolutions per second (RPS) of the impeller.

The relationship between the velocity of the moving fluid and the RPS of a stationary flowmeter measurement, the response curve, is shown in Figure C-1. The threshold velocity (V_T) is the velocity of the moving fluid needed to start the impeller spinning. Once the fluid velocity exceeds V_T, the measured RPS will increase linearly with the fluid velocity. The slope of this response curve is dependent on the borehole diameter and is significantly affected by the viscosity of the moving fluid. In addition, V_T can vary somewhat with the adjustment of the impellor shaft bearings and the fluid properties. This impeller flowmeter measures fluid velocity in a single-phase flow under turbulent conditions, and when centralizers are used to keep the flowmeter in the center of the hole it will measure the maximum velocity of the moving fluid, and a correction factor must be used to obtain the average velocity.

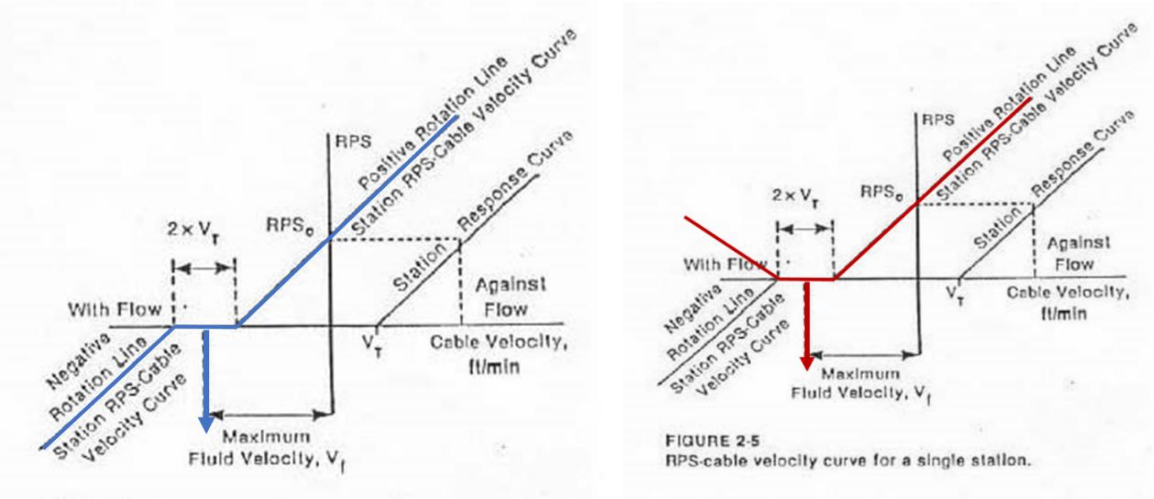

Figure C-1: The difference in RPS output for a flowmeter that has polarity on the left and a flowmeter without polarity on the right.

Collecting multiple logs in both the upward and downward directions allows the detection of smaller flow rates (Crowder & Mitchell, 2002). This helps to understand that the RPS value will be affected differently if the flowmeter is moving with or against the fluid flow. It

is recommended that 3 or more logs be collected (email from Mount Sopris). When the cable velocity (i.e., the velocity of the tool) increases in the direction against fluid flow, the RPS value increases, but when the cable velocity increases in the direction of fluid flow the RPS decreases. This behavior is used in the calibration process to determine the fluid velocity, but the accuracy of the calibration is also dependent on whether or not the flowmeter has polarity (i.e., different signs of the RPS measurement when the impeller spins clockwise or counterclockwise). This is important because when the flowmeter is moving with fluid flow, the RPS will decrease as the tool velocity increases, and when the tool velocity is large enough the RPS reading will be zero, and will remain at zero at higher tool velocities, until the tool velocity becomes large enough to overcome the fluid velocity and cause the impeller to spin in the opposite direction. If the flowmeter does not have polarity, it is difficult to identify when the impeller spin changes. The tool used in HBP5 does not have polarity so no matter which direction the impellor spins it will give a positive output, making it more difficult to quantitatively analyze the flow log.

The patterns of relative changes in flow response show excellent repeatability for the four logs, indicating that using high-resolution flowmeter data is an effective method to identify the position of hydraulically important zones across the borehole (Figure 3-2). However, it is more challenging to perform a quantitative analysis for flow log. The key limitations of quantifying the flow measurements in HBP5 can be summarized below:

1. There is much noise and variability in the flow profile for the upper portion of the open borehole that can be attributed to the extreme downward gradient with large amount of flow entering into the hole from all directions knocking the tool from side to side (the larger tool velocity has even more noise). The noise at the depth where flow is entering the borehole (21.90- 33.67 m bgs) causes the logs to not behave well in that portion of the borehole, making the quantification of the flow log more challenging.

2. It takes time to accurately collect a quantitative flow log and enough time was not given to do this for HBP5 because the hole could not remain open for a long time (due to the impacts of the strong vertical gradient in HBP5 on a nearby private well). Logs were collected at only 2 different speeds from HBP5 but it recommended to conduct at least 3 up/down logs.

3. The first log was downward and very different from the other three logs and therefore, it is likely that the flow in the borehole was not at steady state during the first log. This behavior may also have influenced the second log (2m/min upward).

4. In normal flow conditions, when the probe is moving in the direction of fluid flow the velocity is lower than when it is moving against fluid flow. In HBP5, the same speed is usually seen for different logs indicating that the logs were not collected at a high enough speed.

5. A tool with polarity is the best tool to use to obtain a quantitative flow log because there is no doubt when the impellor spin direction changes. The tool used in HBP5

does not have polarity, and therefore it is difficult to identify when the impellor direction is reversed.

6. Determining V_T in the down hole environment requires delineation of both the positive and negative rotation lines (Figure C-1). Only two stations at the bottom can identify part of the negative rotation line.

7. Stationary measurements are not required, but can be useful to support the estimated value obtained by the y-intercept of the station response curve. No stationary measurements were collected in HBP5

D Appendix D: FEFLOW Input Parameters

Model inputs informing the FEFLOW model include bulk hydraulic conductivity, recharge (elemental parameters), and specified head (nodal parameter). This appendix shows the distribution of these properties across the model layers after calibration. Figure D-1 to Figure D-7 show the distribution of hydraulic conductivity for each model layer.

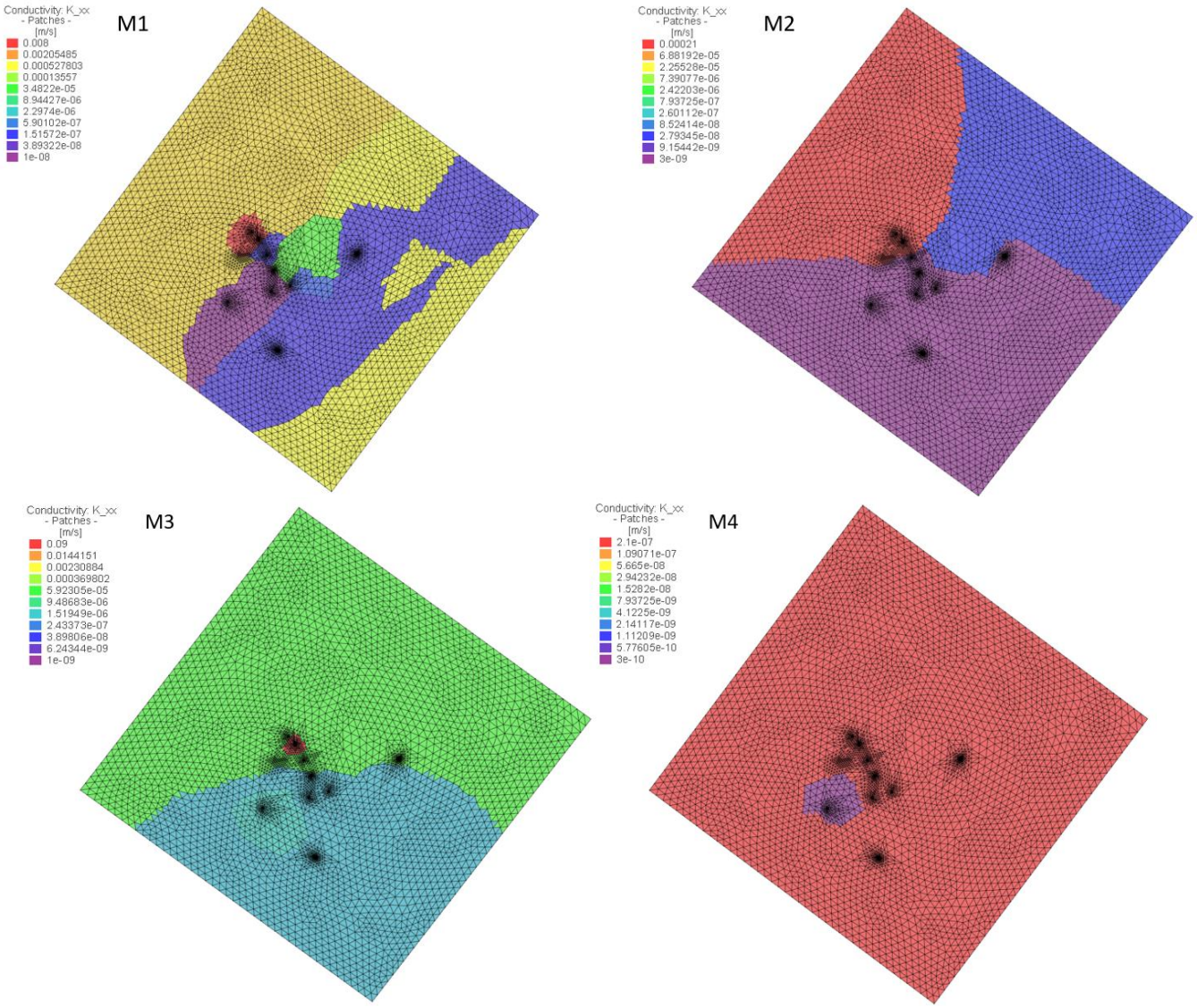

Figure D-1: The distribution of horizontal K_b across layers 1-4.

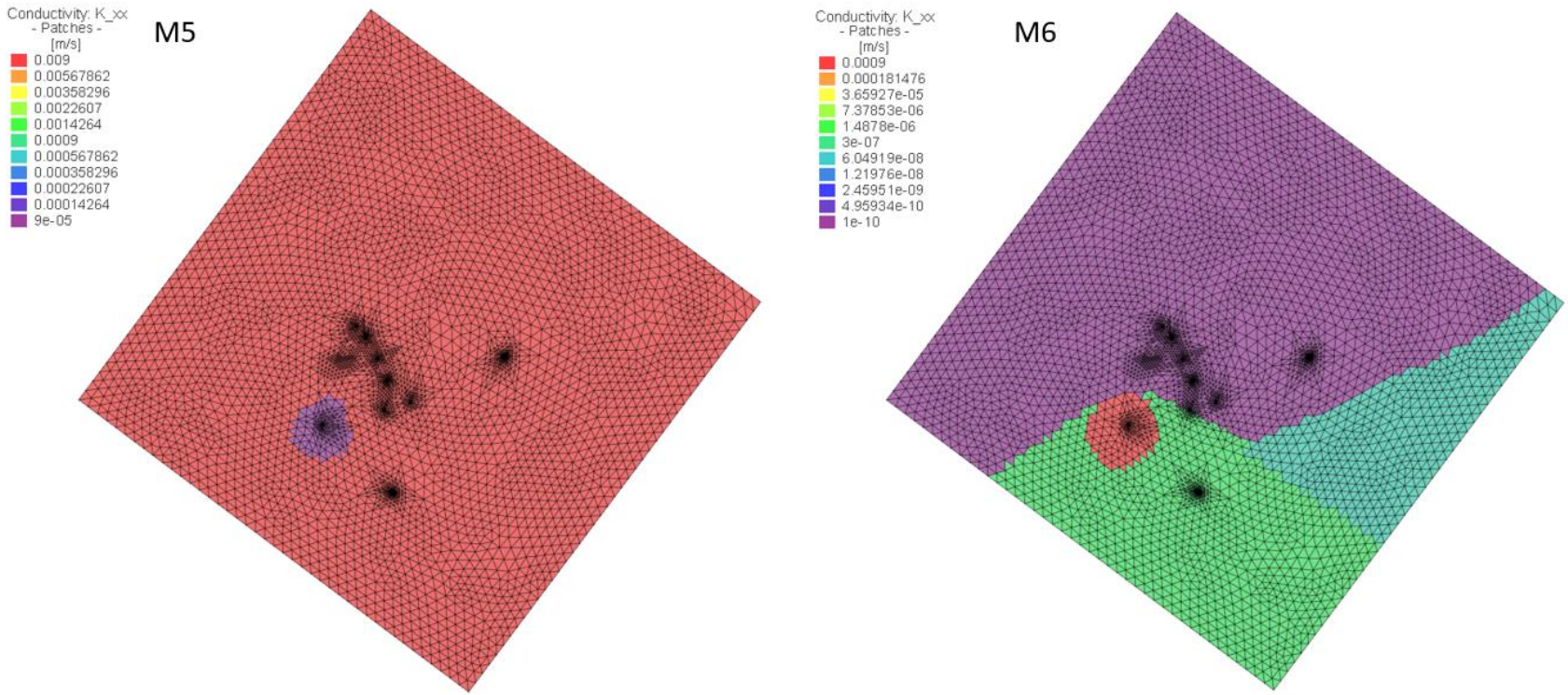

Figure D-2: The distribution of horizontal K_b across layers 5 and 6.

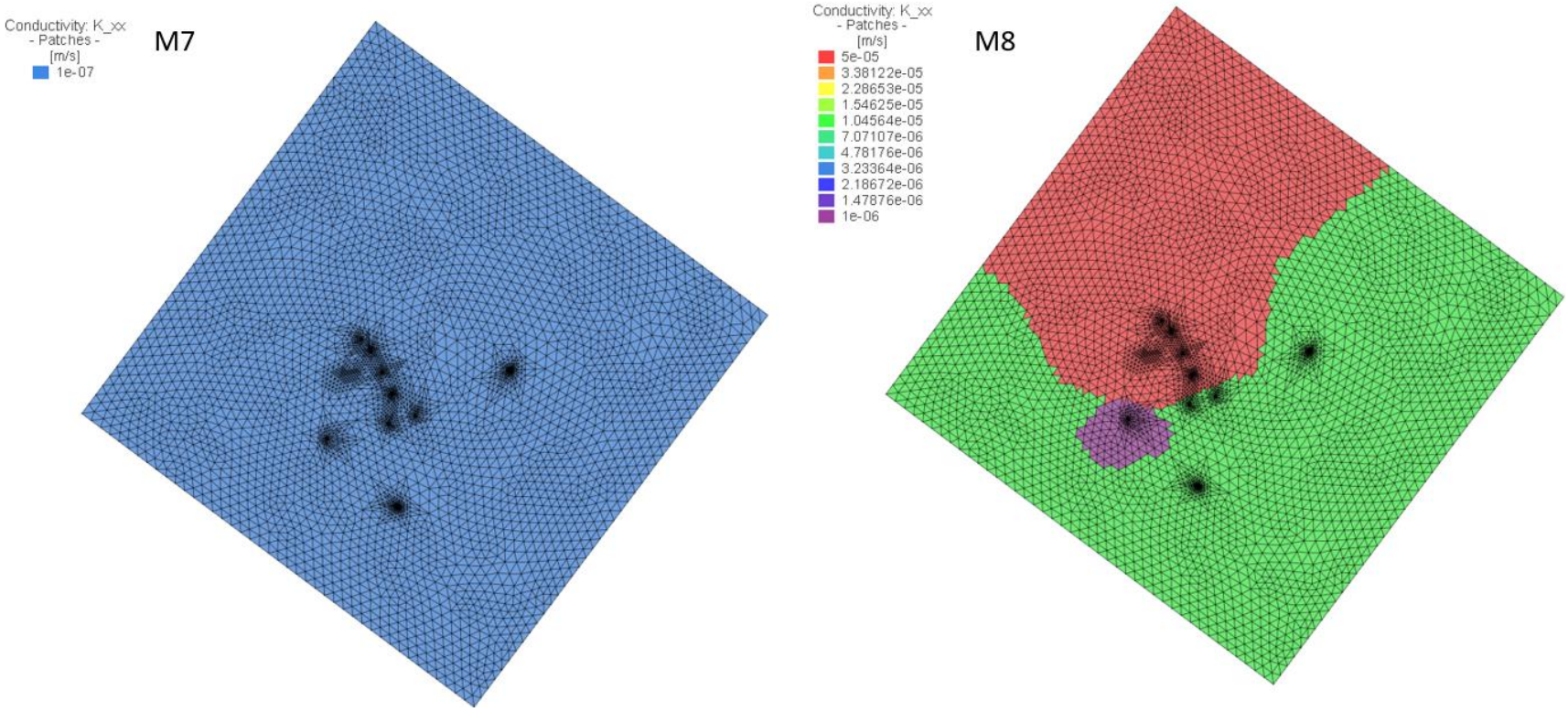

Figure D-3: The distribution of horizontal K_b across layers 7 and 8.

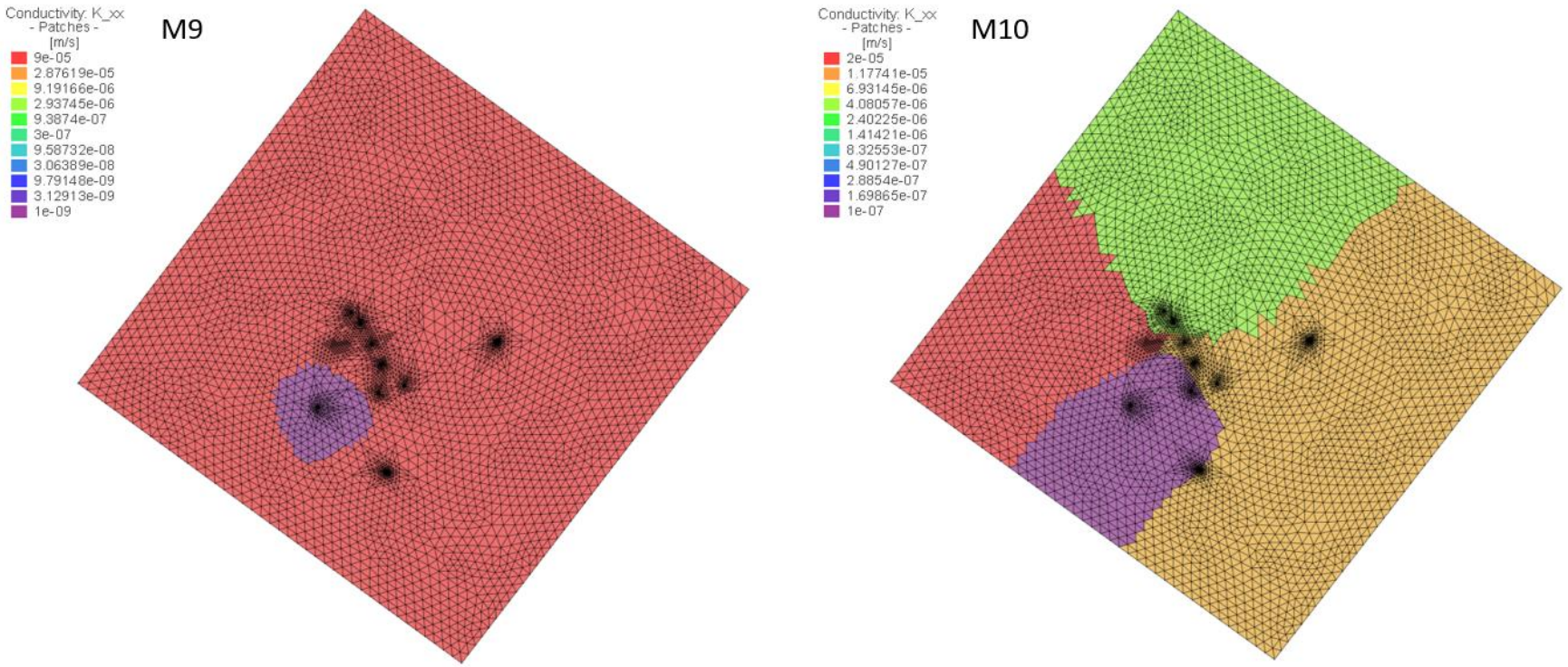

Figure D-4: The distribution of horizontal K_b across layers 9 and 10.

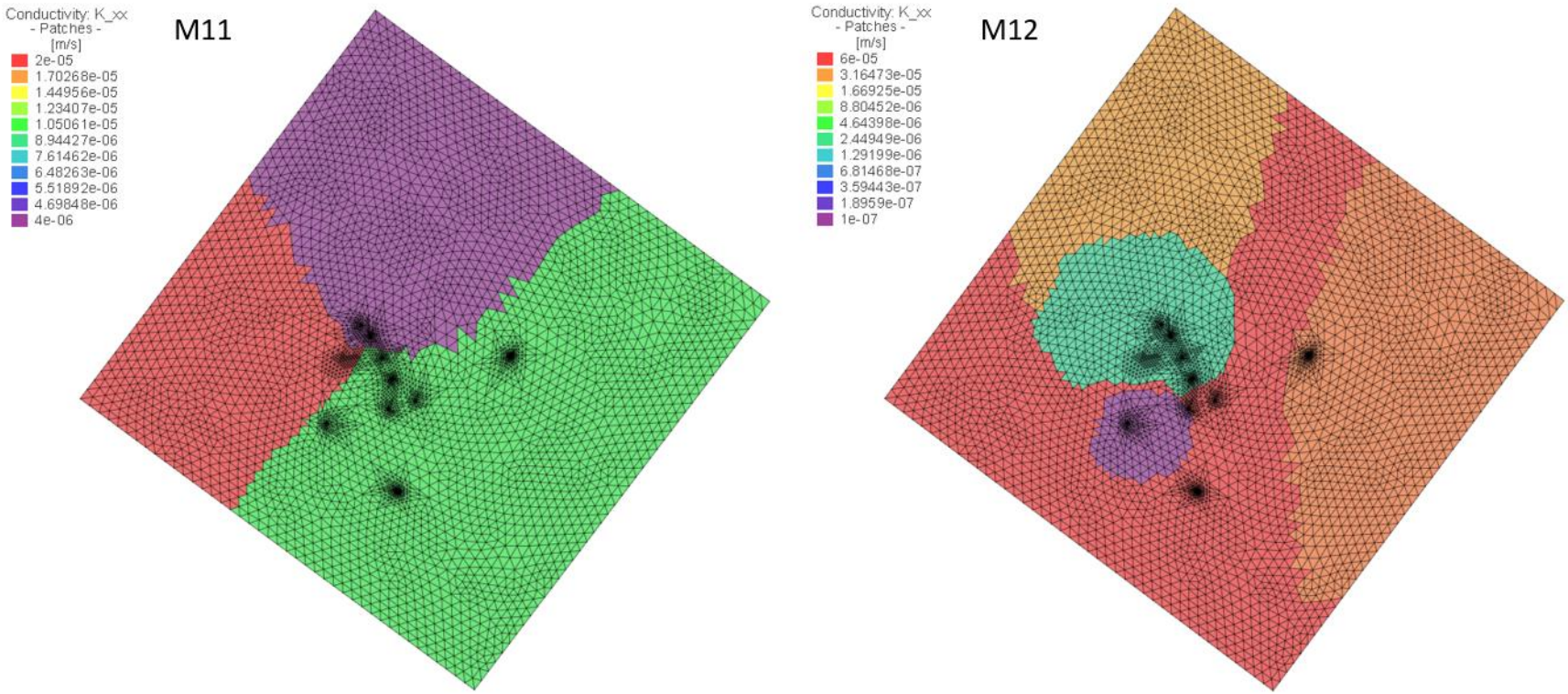

Figure D-5: The distribution of horizontal K_b across layers 11 and 12.

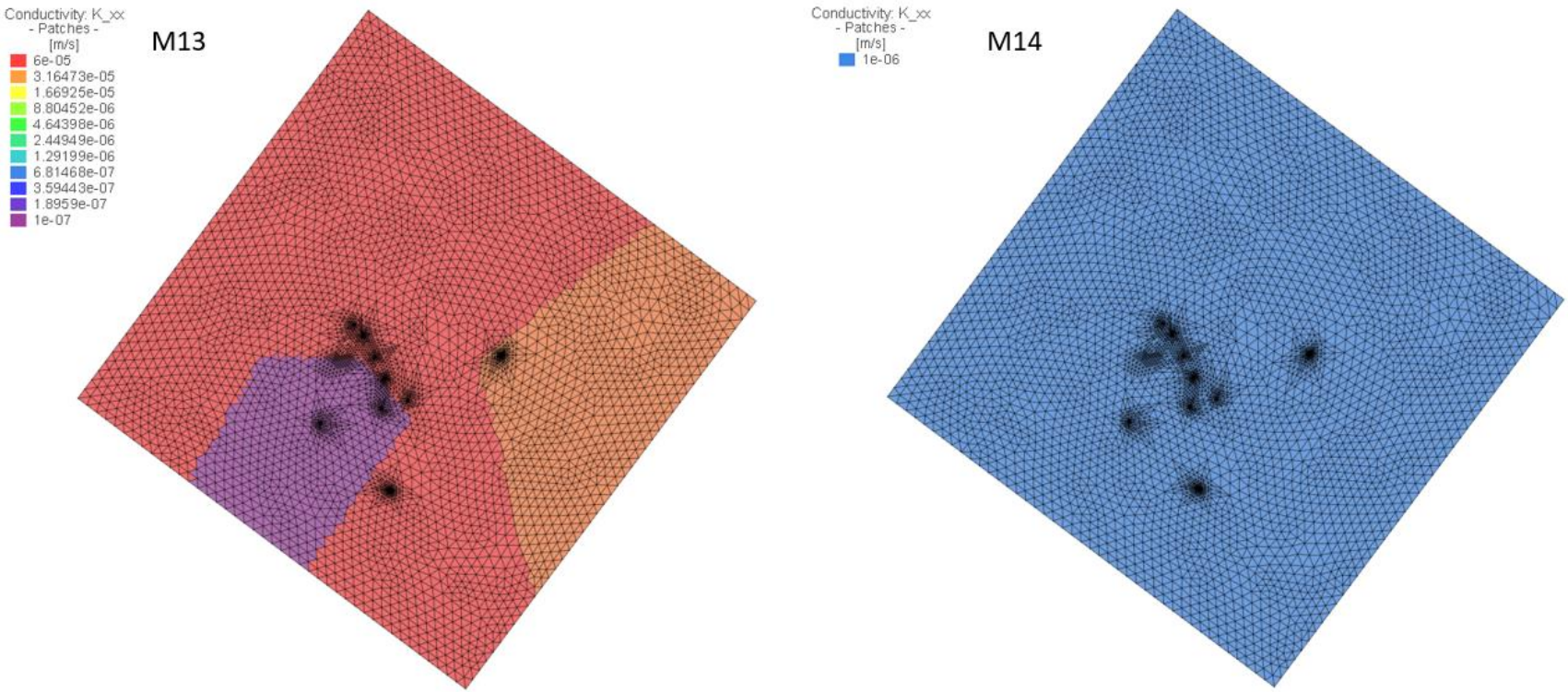

Figure D-6: The distribution of horizontal K_b across layers 13 and 14.

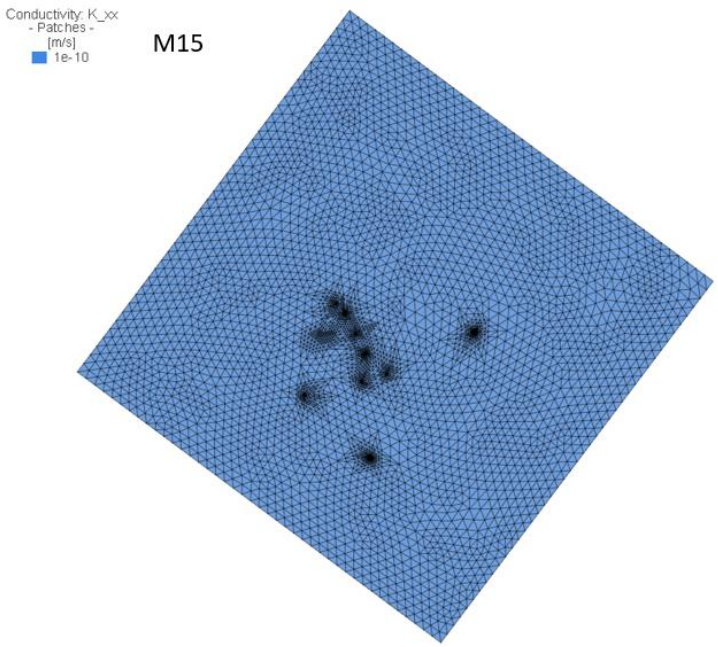

Figure D-7: The distribution of horizontal K_b across layer 15.

Figure D-8 shows the calibrated recharge rates are relatively consistent with the optimized values from the average annual groundwater recharge from the regional model developed by the GAWSER model (Matrix Solutions Inc., 2017).

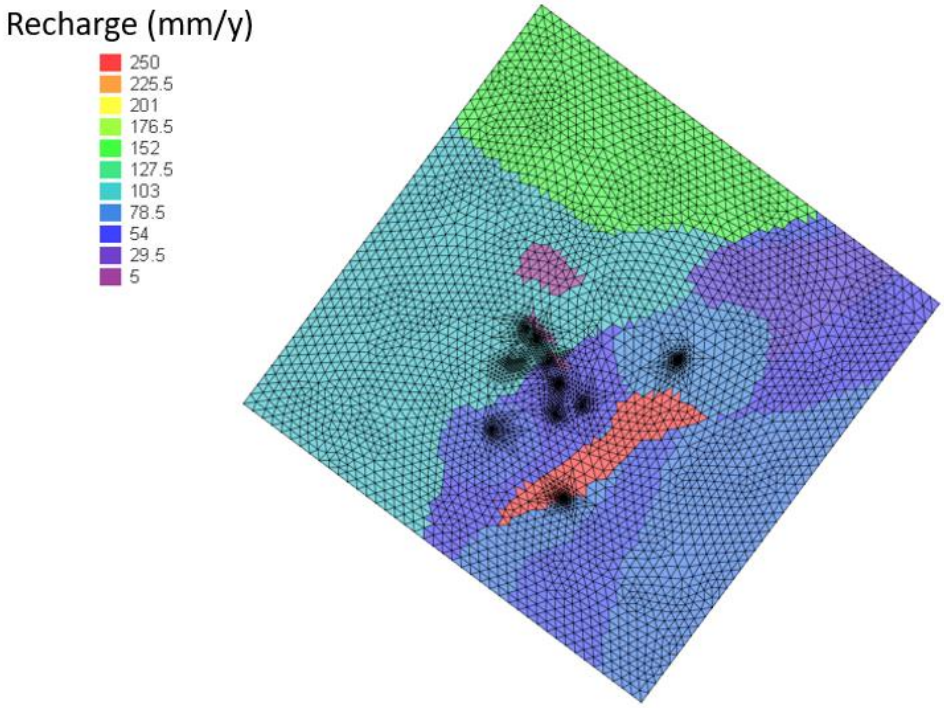

Figure D-8: The calibrated recharge map (mm/y)

The plan view in Figure D-9 shows the model layer for the shallow system on the right and the deep aquifer (Gasport) on the left along with the specified head nodes. Regional potentiometric maps on the same layers are shown in the top right-hand corner (Matrix Solutions Inc., 2017). It is seen that the boundary condition parameters of the cutout model have been set up to be a combination of no flow and specified head to be consistent with the regional model.

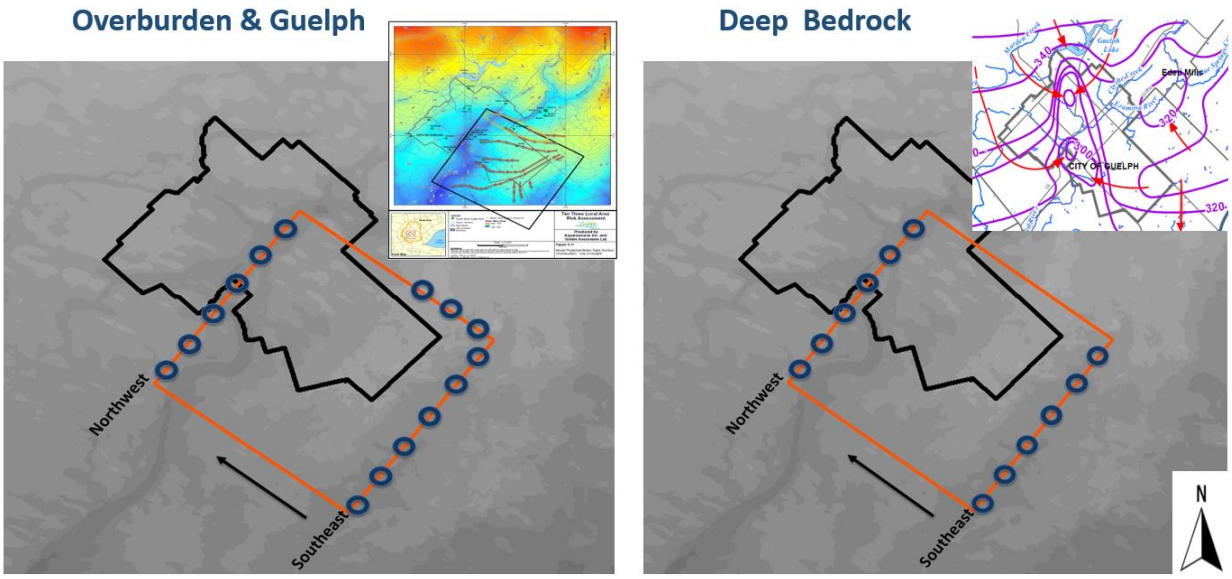

Figure D-9: Specified head nodes on model layers have been set up to be consistent with the regional model.

The simulated potentiometric maps under ambient conditions (no open borehole) are shown for 3 model layers (M5, M7, M12) in Figure D-10 and Figure D-11.

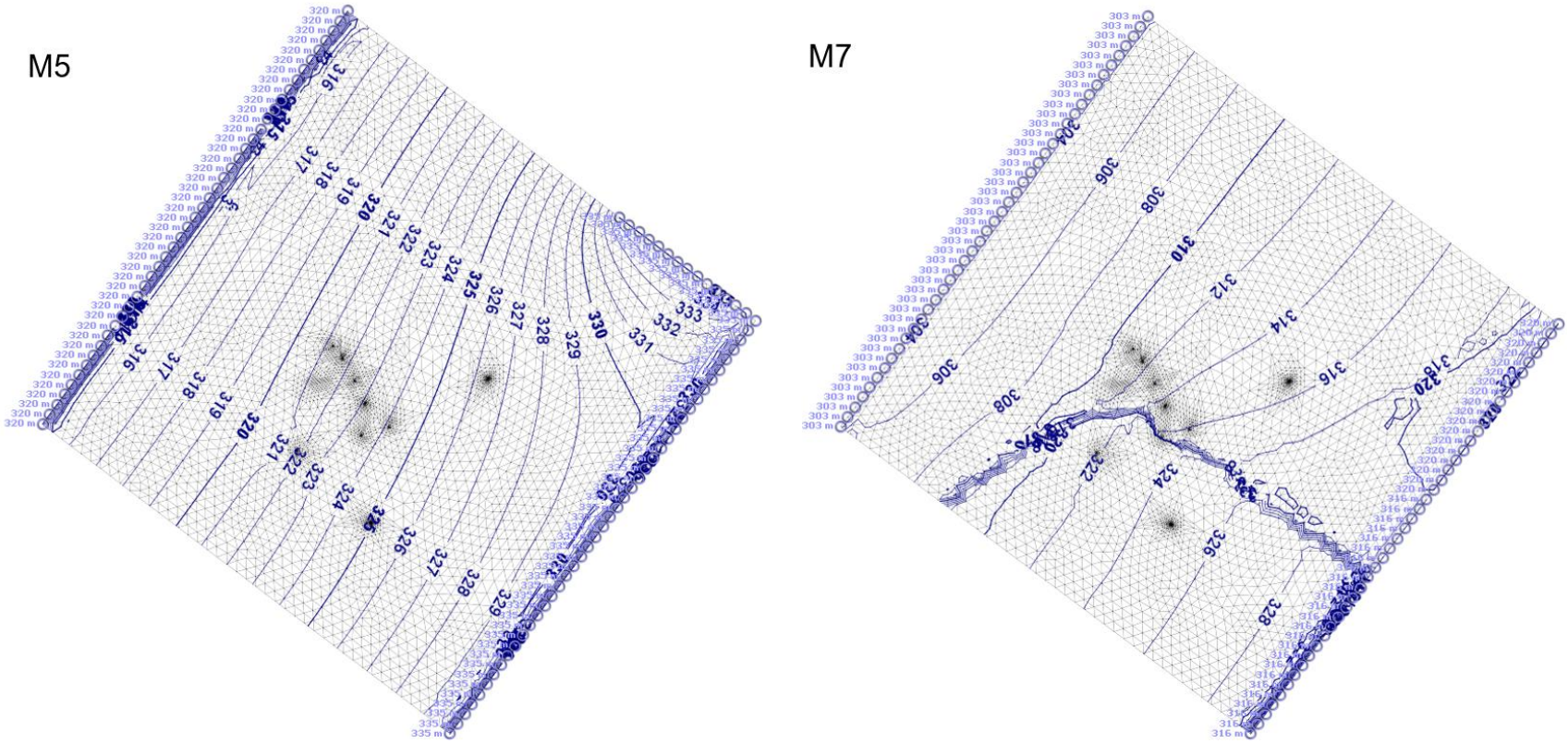

Figure D-10: Predicted potentiometric surfaces (m asl) on layer 5 (left side) and layer 7 (right side).

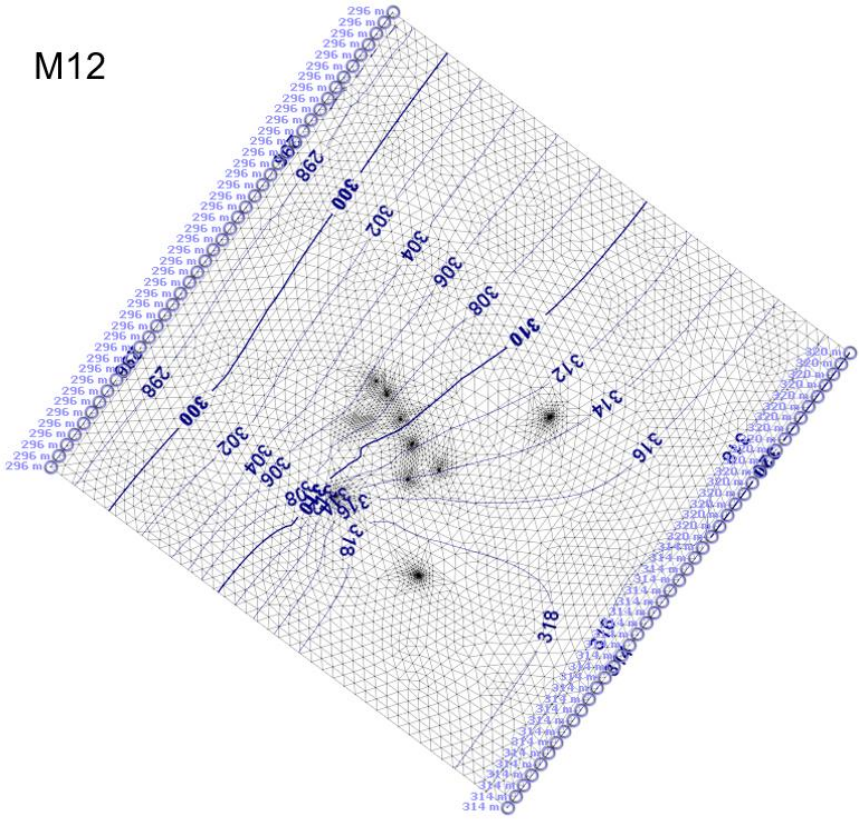

Figure D-11: Predicted potentiometric surfaces (m asl) on layer 12 (middle Gasport aquifer)

Relative sensitivity analysis for recharge and specified heads:

Relative sensitivity of recharge showed that changes in recharge rates had more impacts on the hydraulic heads in the shallow system than those in the bedrock (Figure D-12). R_OB means how changes in recharge impact the hydraulic heads across the overburden and R shows that influence for the heads across the bedrock. Figure D-13 shows the relative sensitivity of heads to changes in specified heads.

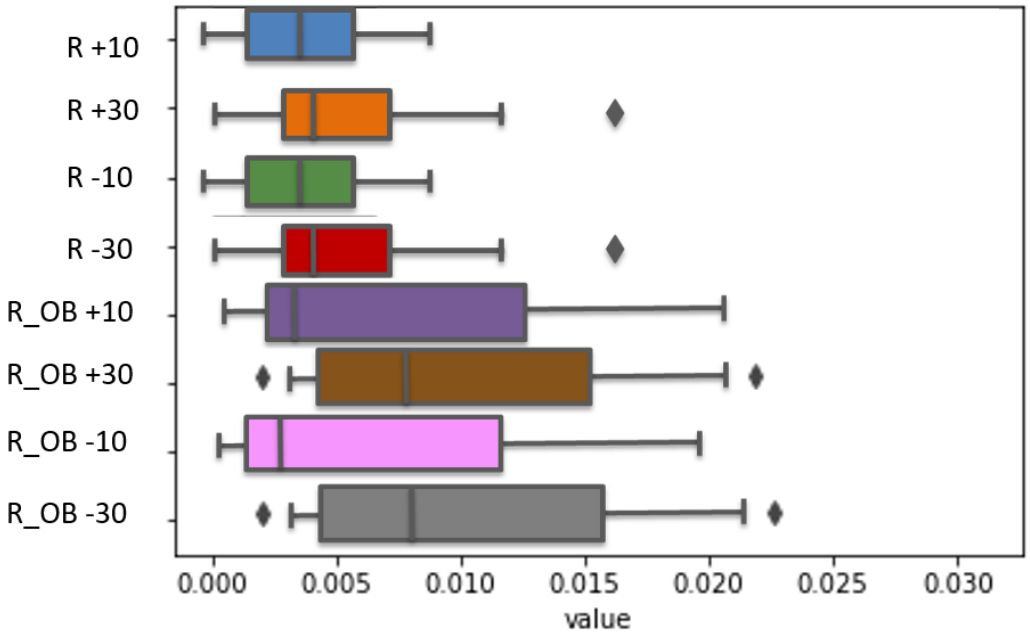

Figure D-12: Relative sensitivity of the heads to changes in recharge.

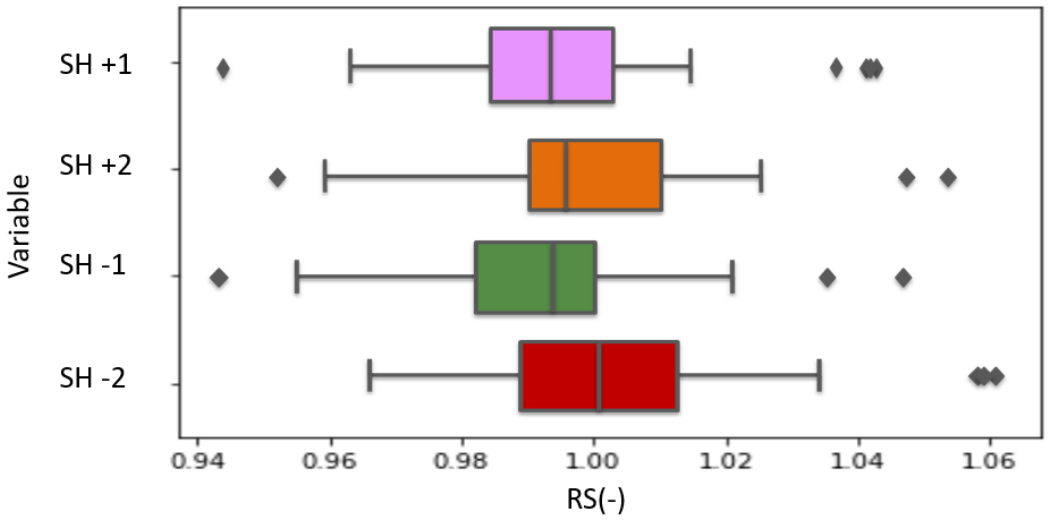

Figure D-13: Relative sensitivity of the heads to changes specified head nodes.

E Appendix E: Regional Tier Three Model- Relevant Details

This appendix contains information from the regional model (Matrix Solutions Inc., 2017) that was used to inform the cutout model. The drilling locations and the details (bedrock) for the regional study are shown in Figure E-1 and Table E-1.

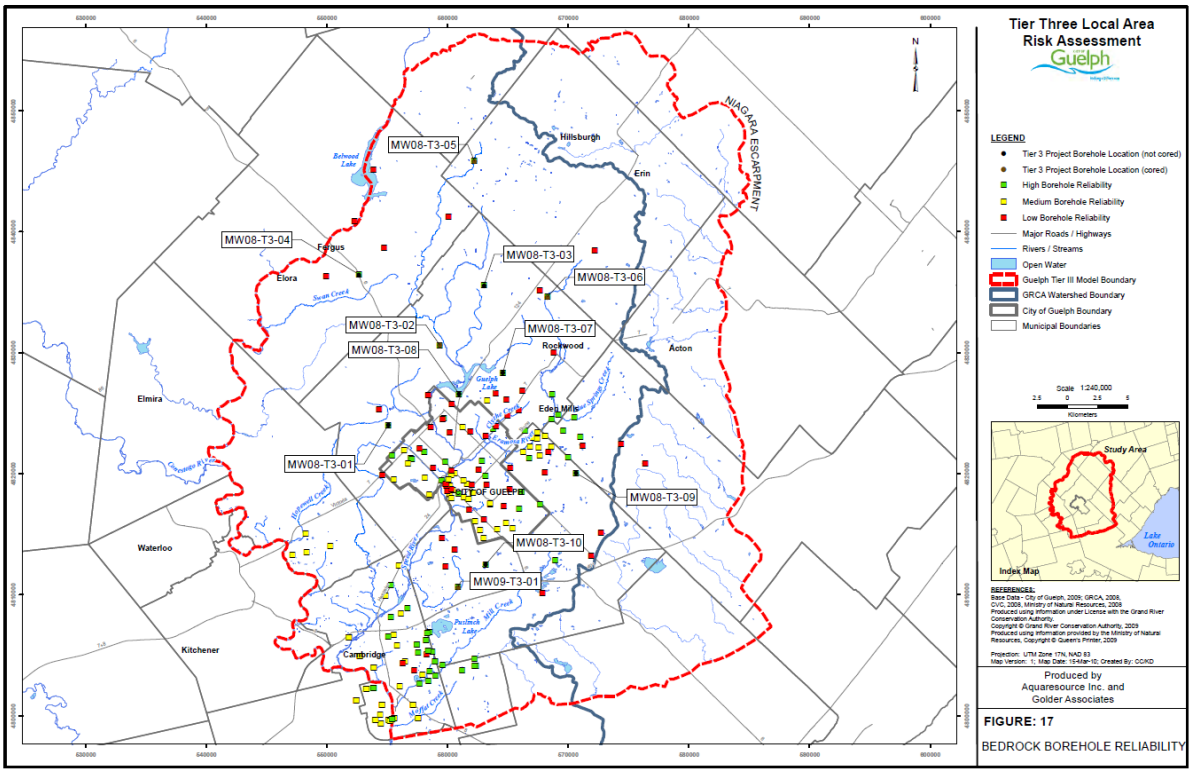

Figure E-1: Tier Three drilling locations

Table E-1: Berdock boreholes geological summary

Formation	MW08-T3-01			MW08-T3-02			MW08-T3-03			MW08-T3-04			MW08-T3-05			MW08-T3-06		
	Top (mbgs)	Bottom (mbgs)	Thickness (m)	Top (mbgs)	Bottom (mbgs)	Thickness (m)	Top (mbgs)	Bottom (mbgs)	Thickness (m)	Top (mbgs)	Bottom (mbgs)	Thickness (m)	Top (mbgs)	Bottom (mbgs)	Thickness (m)	Top (mbgs)	Bottom (mbgs)	Thickness (m)
Overburden	0.0	9.8	9.8	0.0	8.5	8.5	0.0	44.1	44.1	0.0	19.2	19.2	0.0	19.2	19.2	0.0	1.1	1.1
Guelph Formation	not present			8.5	14.6	6.1	not present			19.2	50.0	30.8	not present			not present		
Eramosa Formation (Stone Road Member)	not present			14.6	20.6	6.0	30.5	44.1	13.6	not present			19.2	22.8	3.6	not present		
Eramosa Formation (Reformatory Quarry Member)	9.8	57.9	48.2	20.6	25.3	4.7	44.1	47.4	3.3	not present			22.8	31.4	8.6	not present		
Eramosa Formation (Vinemount Member)	57.9	58.5	0.6	25.3	31.4	6.1	47.4	54.3	6.9	not present			31.4	33.7	2.3	not present		
Goat Island Formation (Ancaster Member)	58.5	75.1	16.6	not present			not present			not present			not present			1.1	1.5	0.4
Goat Island Formation (Niagara Falls Member)	not present			not present			54.3	66.8	12.5	50.0	90.0	40.0	33.7	53.3	19.6	1.5	6.0	4.5
Gasport Formation	75.1	91.1	16.0	31.4	82.8	51.4	66.8	93.4	26.6	90.0	139.0	49.0	53.3	99.0	45.7	6.0	50.5	44.5
Irondequoit Formation	91.1	92.3	1.2	82.8	84.5	1.7	93.4	95.1	1.7	139.0	139.9	0.9	99.0	100.5	1.5	50.5	51.7	1.2
Rockway Formation	92.3	93.2	0.9	84.5	85.4	0.9	95.1	95.7	0.6	139.9	140.7	0.8	100.5	101.2	0.7	51.7	54.0	2.3
Merritton Formation	93.2	94.5	1.3	85.4	85.9	0.5	not present			140.7	141.4	0.7	101.2	101.7	0.5	not present		
Cabot Head Formation	94.5	95.7	1.2	85.9	89.9	4.0	95.7	97.2	1.5	141.4	143.9	2.5	101.7	104.9	3.2	54.0	57.7	3.7

Formation	MW08-T3-07			MW08-T3-08			MW08-T3-09			MW08-T3-10			MW09-T3-01		
	Top (mbgs)	Bottom (mbgs)	Thickness (m)	Top (mbgs)	Bottom (mbgs)	Thickness (m)	Top (mbgs)	Bottom (mbgs)	Thickness (m)	Top (mbgs)	Bottom (mbgs)	Thickness (m)	Top (mbgs)	Bottom (mbgs)	Thickness (m)
Overburden	0.0	14.9	14.9	0.0	16.0	16.0	0.0	25.6	25.6	0.0	38.5	38.5	0.0	23.8	23.8
Guelph Formation	not present			not present			not present			not present			23.8	38.6	14.8
Eramosa Formation (Stone Road Member)	not present			not present			not present			not present			not present		
Eramosa Formation (Reformatory Quarry Member)	14.9	20.0	5.1	16.0	21.7	5.7	not present			38.5	45.8	7.3	38.6	50.2	11.6
Eramosa Formation (Vinemount Member)	20.0	34.6	14.6	21.7	29.3	7.6	not present			not present			50.2	58.4	8.2
Goat Island Formation (Ancaster Member)	34.6	51.8	17.2	29.3	38.3	9.0	25.6	41.2	15.6	45.8	57.4	11.6	not present		
Goat Island Formation (Niagara Falls Member)	not present			38.3	55.8	17.5	41.2	48.4	7.2	57.4	66.7	9.3	58.4	61.6	3.2
Gasport Formation	51.8	69.8	18.0	55.8	72.8	17.0	48.4	79.1	30.7	66.7	100.9	34.2	61.6	105.2	43.6
Irondequoit Formation	69.8	72.0	2.2	72.8	74.0	1.2	79.1	81.6	2.5	100.9	102.9	2.1	105.2	107.0	1.8
Rockway Formation	72.0	73.2	1.2	74.0	74.5	0.5	81.6	83.2	1.6	102.9	103.5	0.6	107.0	108.0	1.0
Merritton Formation	73.2	75.0	1.8	74.5	75.2	0.7	83.2	84.1	0.9	103.5	105.2	1.7	108.0	109.2	1.2
Cabot Head Formation	75.0	76.5	1.5	75.2	76.2	1.0	84.1	84.7	0.6	105.2	105.4	0.2	109.2	113.1	3.9

Figure E-2 demonstrates the recharge rates on the regional model developed by the GAWSER model in a steady-state mode (Matrix Solutions Inc., 2017). The GAWSER model is a physical model that was used to simulate watershed hydrology and predict the total streamflow resulting from inputs of rainfall and/or snowmelt.

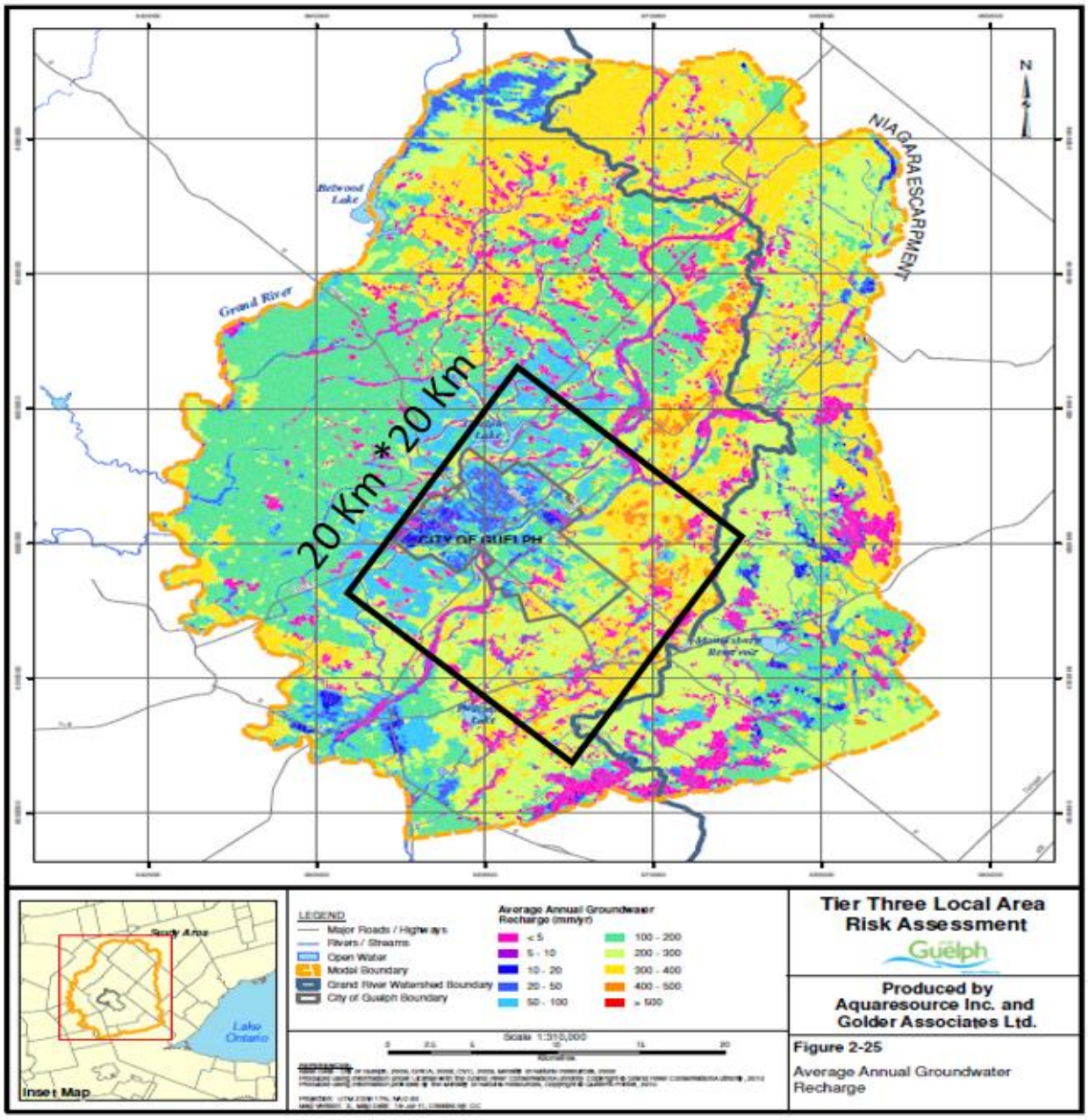

Figure E-2: The regional recharge map (mm/y). The black square shows a domain bigger than the cutout model (double size) to provide a big picture of recharge distribution

Figure E-3 and Figure E-4 show the regional potentiometric surfaces for the overburden and Gasport aquifer, respectively. These data were used to inform the boundaries of the cutout model.

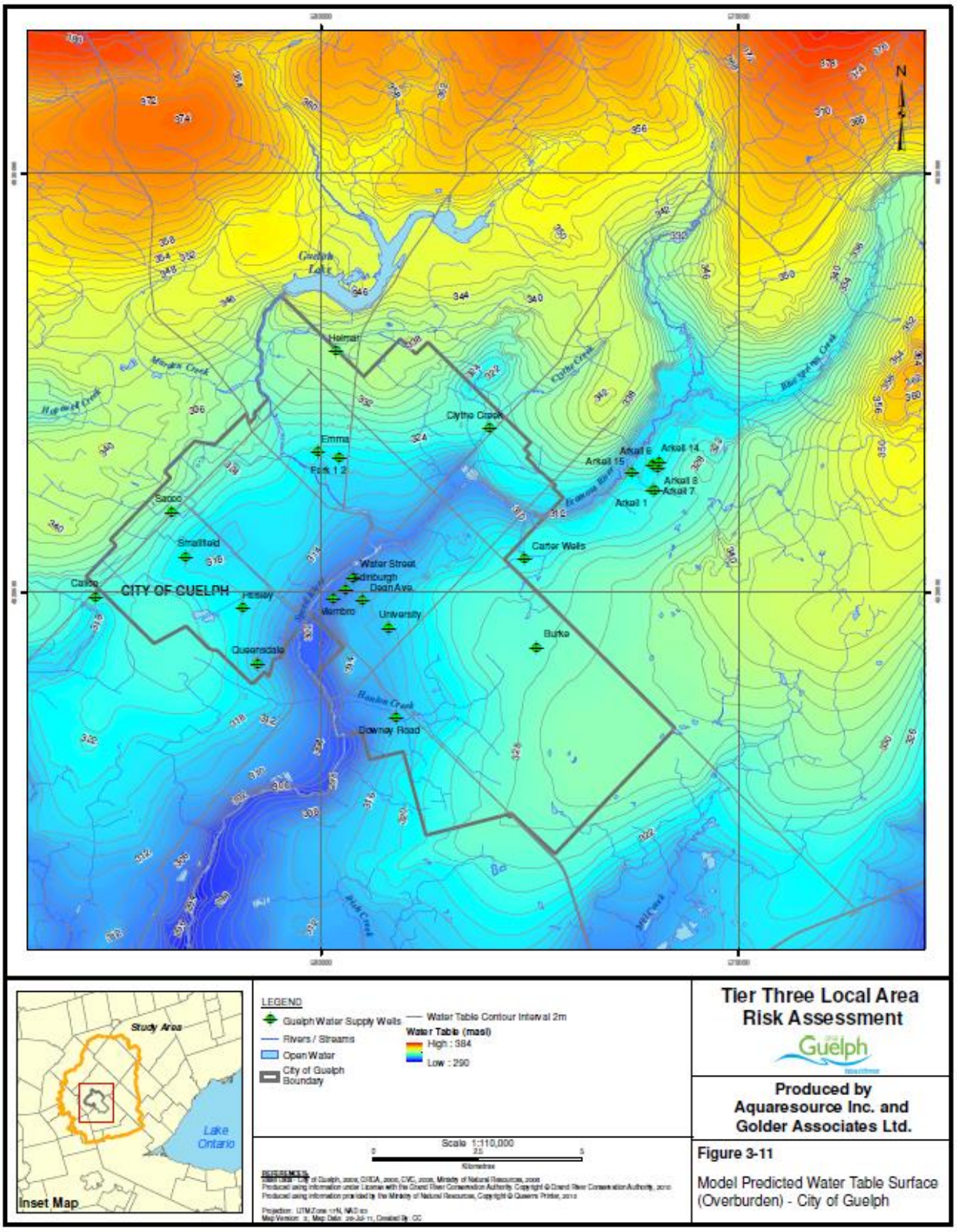

Figure E-3: Simulated potentiometric surfaces (overburden)- Regional map

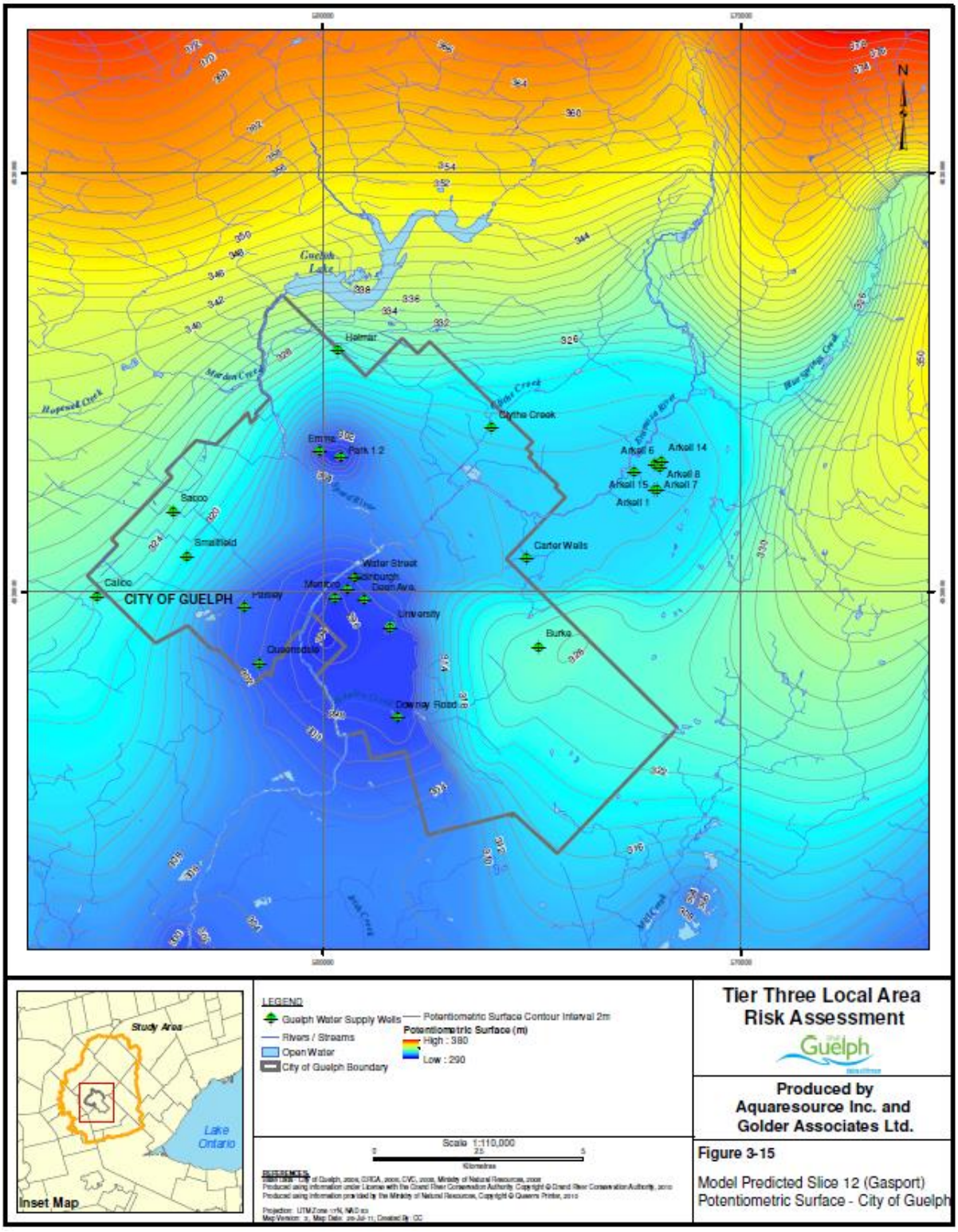

Figure E-4: Simulated potentiometric surfaces (Gasport aquifer)- Regional map